

**NASA CONTRACTOR
REPORT**

NASA CR-2075



NASA CR-2
21

0061201



LOAN COPY: RETURN TO
AFWL (DOUL)
KIRTLAND AFB, N. M.

**RESIDUAL STRENGTH AND CRACK
PROPAGATION TESTS ON
C-130 AIRPLANE CENTER WINGS
WITH SERVICE-IMPOSED FATIGUE DAMAGE**

*by H. Lawrence Snider, Franklin L. Reeder,
and William Dirkin*

Prepared by
LOCKHEED-GEORGIA COMPANY
Marietta, Ga. 30060
for Langley Research Center





0061201

1. Report No. NASA CR-2075		2. Government Accession No.		3. Recipient's Catalog No.	
4. Title and Subtitle RESIDUAL STRENGTH AND CRACK PROPAGATION TESTS ON C-130 AIRPLANE CENTER WINGS WITH SERVICE-IMPOSED FATIGUE DAMAGE				5. Report Date July 1972	
				6. Performing Organization Code	
7. Author(s) H. Lawrence Snider, Franklin L. Reeder, and William Dirkin				8. Performing Organization Report No. ER 11178	
9. Performing Organization Name and Address Lockheed-Georgia Company Marietta, Ga. 30060				10. Work Unit No. 126-14-15-01	
				11. Contract or Grant No. NAS 1-9485	
12. Sponsoring Agency Name and Address National Aeronautics and Space Administration Washington, D.C. 20546				13. Type of Report and Period Covered Contractor Report	
				14. Sponsoring Agency Code	
15. Supplementary Notes Supplementary information available in NASA CR 112008					
16. Abstract Fourteen C-130 airplane center wings, each containing service-imposed fatigue damage resulting from 4000 to 13000 accumulated flight hours, were tested to determine their fatigue crack propagation and static residual strength characteristics. Eight wings were subjected to a two-step constant-amplitude fatigue test prior to static testing. Cracks up to 30 inches long were generated in these tests. Residual static strengths of these wings ranged from 56 to 87 percent of limit load. The remaining six wings containing cracks up to 4 inches long were statically tested as received from field service. Residual static strengths of these wings ranged from 98 to 117 percent of limit load. Damage tolerant structural design features such as fastener holes, stringers, doublers around door cutouts, and spanwise panel splices proved to be very effective in retarding crack propagation.					
17. Key Words (Suggested by Author(s)) Full-scale aircraft wings Fatigue crack propagation Static residual strength				18. Distribution Statement Unclassified - Unlimited	
19. Security Classif. (of this report) Unclassified		20. Security Classif. (of this page) Unclassified		21. No. of Pages 67	22. Price* \$3.00

RESIDUAL STRENGTH AND CRACK PROPAGATION TESTS
ON C-130 AIRPLANE CENTER WINGS
WITH SERVICE-IMPOSED FATIGUE DAMAGE

H. Lawrence Snider, Franklin L. Reeder, and William Dirkin

Lockheed-Georgia Company

SUMMARY

Fourteen C-130 airplane center wings with 4,000 to 13,000 flight hours and associated fatigue damage were tested to destruction. Six wings were tested for static residual strength as received from field service. The other eight wings were tested in crack propagation cyclic testing at a prescribed stress level for 10,000 cycles, or less. Then the stress level was reduced, and testing to a maximum of 20,000 total cycles was conducted. Testing was performed with constant-amplitude stress at a stress ratio of 0.1. Maximum cyclic stresses were approximately 18,000 psi. At the conclusion of cyclic testing, a static residual strength test was conducted.

Static residual strength of the specimens as received (without prior test cycling) ranged from 98 percent to 117 percent limit load. Some of these specimens had initial crack lengths of 4.0 inches or more. The theoretical (Miner's expression) fatigue damage experienced by these wings during flight service ranged from .61 to 1.26; there was no evident correlation between service-imposed fatigue damage and static residual strength.

The static residual strength of the wings which had been subjected to up to 20,000 crack propagation test cycles ranged from 56 percent to 87 percent limit load. Some specimens had cracks greater than 30 inches at the conclusion of cyclic testing. Theoretical calculations (Miner's expression) of fatigue damage imposed by test cycling ranged as high as 7.

Several damage tolerant structural design features proved to be effective in retarding crack propagation. The fastener holes in the skin occasioned by the "built-up" type

of wing construction were quite effective, as there were many instances of fatigue cracks entering into, and then residing in, fastener holes or stopdrilled holes for thousands of load cycles. Reinforcements such as stringers and doublers around door cutouts consistently arrested the growth of skin cracks by re-distribution of stresses near the crack tips, even when corner cracks had initial lengths greater than 4.0 inches. The spanwise splices associated with the use of multiple spanwise skin panels repeatedly arrested or retarded crack propagation.

The number of instances in which the largest initial cracks failed to propagate appreciably under cyclic testing, with eventual failure occurring elsewhere, was unexpectedly high.

Most fatigue cracks started at fastener holes near major structural discontinuities, including termination of reinforcement of corners of cutouts, and rib attachments to skin.

INTRODUCTION

Detailed information is needed concerning the effect of actual service conditions, particularly service-imposed fatigue damage, on the strength of representative types of aircraft wing structures. As an aircraft is used it accumulates fatigue damage, often at an increasing rate. As fatigue cracks in the aircraft grow longer, generally their rate of propagation and the associated risk of catastrophic fatigue failure increases, thereby requiring more frequent and thorough inspections and repairs so that the airplane's safety and reliability are maintained. A definite need exists for experimental strength data for typical airframe construction which has been subjected to prior service-imposed fatigue damage, and to obtain these data under realistic test conditions. This program was directed to achieve these objectives by generating experimental data which include both residual strength and crack propagation behavior from tests performed on fourteen C-130 wing boxes which have been subjected to service operation.

Center wing boxes became available for these tests consequent to a wing modification program being conducted on C-130B and E series aircraft in which the original service-

damaged center wing boxes were replaced with an improved version. The availability of these old center wing sections, which have experienced substantial service-imposed fatigue damage, provides a unique opportunity to conduct crack propagation and residual strength tests to evaluate strength and fatigue performance in terms of service history, location and length of cracks, construction details, damage tolerant design features, load levels, rates of crack propagation under cyclic or increasing static loading, and other relevant parameters.

Detailed records of the service and environmental experiences of each aircraft, along with visual inspection of the structure, comprised the basis for selection of test specimens and for correlation with test results. The hundreds of center wing boxes removed from the aircraft during the current C-130 wing modification program provided a wide range of selection of test specimens which had varied types of fatigue damage.

The following tests were conducted:

- (a) Three upbending tests for static residual strength evaluation (without prior test cycling).
- (b) Four upbending tests for crack propagation cyclic testing at a maximum of 10,000 cycles at one load level, followed by testing at a reduced load level to a maximum total of 20,000 cycles. Static residual strength tests were conducted at the conclusion of cyclic testing.
- (c) Three downbending tests for static residual strength evaluation (without prior test cycling).
- (d) Four downbending tests for crack propagation cyclic testing at a maximum of 10,000 cycles at one load level, followed by a maximum of 10,000 cycles at a reduced load level. Static residual strength tests were conducted at the conclusion of cyclic testing.

All cyclic testing was conducted with constant amplitude stress at a stress ratio of $R = 0.1$. Maximum cyclic loading applied was 50 percent of limit load, which results in nominal tensile stresses of approximately 18,000 psi over a large portion of the wing surface.

The principal data gathered from the static residual strength tests involve initial crack length, growth of cracks with increasing load levels, the effect of local construction

details on crack growth, and residual strength level. Additional information was collected from the cyclic tests. Data on relationships among crack propagation; load level, and number of cycles were gathered. The location and extent of initial damage, major fatigue test damage, and residual static strength level were recorded. The effectiveness of several types of damage tolerant design features in retarding crack growth was observed, including fastener or stopdrilled holes, reinforcing doublers and stringer flanges, and spanwise panel splices.

Service utilization history of the test specimens has been compiled from flight monitoring programs, and enables correlation among airplane usage, initial damage, and experimental cyclic and static test results. The total information gathered from this program is expected to contribute substantially to the formulation of a method for estimating the remaining service life and residual strength of fatigue damaged structure.

The very large quantity of test data gathered is included in Reference 1, along with details of flight service history of the airplanes from which the center wing box test specimens were removed.

An 18 minute, narrated, color motion picture film was made of the test program.

Several terms which are used repeatedly throughout the text are defined in the Appendix.

TECHNICAL APPROACH

Description of Wing Structure

The structural configuration of the C-130 center wing box is illustrated in Figures 1, 2, 3, and 4. Gross dimensions of the center wing box are 440 inches span, 80 inches chord, and 32 inches depth. Each wing box weighs approximately 3800 lbs.

The upper surface of the wing box is composed of four panels. Each panel is approximately 440 inches in span and 20 inches in chord, and is fabricated from machined 7178-T6 aluminum extrusions which have six integral risers spaced at 3.3 inch intervals.

Each of these panels is further stiffened by the installation of three spanwise stringers made from 7178-T6 extruded hat sections spaced at 6.6 inch intervals and installed with riveted attachments except at the spanwise splices. The spanwise splices are butt joints with an extended leg of a hat section stiffener forming a splice plate and fastened with steel lockbolts. Basic upper surface skin thickness of the machined panel is 0.100 inch for the entire span of the center wing. The principal structural discontinuities, which are illustrated in Figure 3, occur approximately symmetrically in both wings, and are at the transition structure immediately inboard of the W. S. 220 production joint; at the W. S. 180 access door cutout; the W. S. 120.5 fuel filler cap opening, and at the inboard (W. S. 105) and outboard (W. S. 135.5) ends of its reinforcement doubler; at the W. S. 61.5 wing-fuselage support rib; and at the dry bay access door cutout at W. S. 1.5 and the ends of its reinforcing doubler at W. S. 34.5/37.5. These are the locations where most of the upper surface fatigue cracks originated during service.

The lower surface is composed of three panels. Each panel is approximately 440 inches in span and 26.7 inches in chord, and is fabricated from chem-milled 7075-T6 plate with extruded 7075-T6 hat section stiffeners located at 5.70 inch spacing. The spanwise splices and attachments for the lower surface are similar to those for the upper surface. Lower surface skin thickness of the machined panel is 0.155 inches in the center region between W. S. 68L and W. S. 68R, tapers from 0.155 inches at W. S. 68 (both wings) to 0.092 inches at W. S. 179, and remains at 0.072 inches to W. S. 220. The principal structural discontinuities, which are illustrated in Figure 4 and which occur approximately symmetrically in both wings, are in the transition structure immediately inboard of the W. S. 220 production joint; at the W. S. 120.5 fuel bag access door; and at the ends of the reinforcing I-beam (W. S. 181/176 and W. S. 58) and doubler (W. S. 168 and 73.0) which extend past both sides of the W. S. 120.5 fuel bag access opening.

Wing cross-section geometry is shown in Figure 2. The front and rear spars are composed of 7075-T6 aluminum extruded caps with 7075-T6 webs; except in the areas of the nacelle the webs are 301 Full Hard, 17-7PH, or AM 350 stainless steel (dependent on specific aircraft serialization).

Applied Loads and Stresses

Loads were applied as illustrated in Figure 5. Shear and bending moments are applied at both ends of the beam (W. S. 220R and 220L) and reacted by balancing forces at W. S. 61L and 61R. Torsion is generated by applying the resultant shear forces at prescribed chordwise locations at W. S. 220L and 220R. Magnitudes of all three applied loading conditions are listed in Table 1. Further details are given in Reference 1.

Applied loading conditions for crack propagation test cycling were nearly identical to the conditions applied in the C-130E TAC Wing Fatigue Test, which was a full-scale airplane fatigue test program conducted earlier on the C-130 Project. For upbending, the shape of the bending moment diagram for the C-130E TAC Wing Fatigue Test is nearly identical to that for allowable static ultimate strength, so this loading condition was used for all upbending testing both cyclic and static. For downbending, the shapes of the bending moment diagrams for the C-130E TAC Wing Test and for allowable static ultimate strength are different, so separate test loading conditions were used for static and cyclic testing to represent the appropriate airplane loading conditions. Condition D-1 was used for all downbending cyclic tests and for the residual strength test of Specimen #6. Condition D-2 was used for the residual strength tests of Specimens #7, #8, #9, #10, #11, and #12. Reference 1 provides complete details on the applied loading conditions.

Approximate wing skin stresses (spanwise) on the tension surface for each of the three test loading conditions are shown in Figure 6 for 150 percent Limit Load (ultimate design load) and 50 percent Limit Load. All cyclic crack propagation testing was conducted at 50 percent Limit Load or less. The stresses shown are nominal values at each span station, and do not reflect some chordwise variation in stress due to small changes in wing depth or the effects of local structural discontinuities or stress concentrations.

Cyclic Test Load Levels

Fracture mechanics calculations for cracked plates shown in Table 2 were used to establish initial cyclic load levels for each test. Very little crack propagation resulted when these calculated load levels were applied to the first few specimens. In order to obtain meaningful crack propagation data, initial cyclic load levels on subsequent tests were adjusted on the basis of the crack propagation behavior of preceding specimens. Obviously the simplified fracture mechanics calculations did not account for the many structural design features which effectively resist crack growth.

Flight Service Experience

The flight hours accumulated on each center wing box are shown in Tables 3 and 4. The twelve military aircraft were flown on nine types of missions. The number of flight hours for each type of mission for each airplane; a definition of each mission in terms of flight time versus altitude, airspeed, fuel, and cargo; and other related flight service experience details and fatigue damage information are given in Reference 1. A description of the utilization of the two commercial airplanes from which wing boxes #13 and #14 were removed is also given. From this background information a theoretical comparison of the severity of fatigue damage caused by flight service versus the fatigue damage caused by test cycling was made for the eight specimens which were test cycled, as shown in Figure 7.

The results from these tests can be used to show that the eight wing box specimens tested in the crack propagation tests could have been used in service considerably longer than they were actually used while maintaining at least the residual strength levels achieved in subsequent static tests and listed in Tables 3 and 4.

Strain Survey

A local strain survey of the internal load distribution resulting from the external loads applied to the wing through the W. S. 220 joints at the ends of the test specimen was conducted on Specimen #14. Strains were read immediately inboard of the W. S. 220

joint for each of the three test loading conditions and for four load conditions of the C-130E Fatigue Test Program (for which a full-length wing test specimen was used). The good correlation among these strains and those from the full-length wing indicates the test loading fixture introduces realistic airplane-type stress-strain distribution at the ends of the specimen at W. S. 220L and W. S. 220R and therefore accurately simulates the stresses throughout the entire wing box.

TEST APPARATUS

DESCRIPTION AND VIEWS OF TEST SYSTEM

Specimen Preparation and Test Procedure

Center wing boxes were tentatively selected for testing based on Air Force field inspection reports of fatigue cracking, and followed by visual inspection to verify or further define the extent of fatigue or cracking in service.

Some wings had repair patches with a surface area of several square feet. These were removed to the extent necessary to obtain meaningful crack propagation data, and the wing restored as nearly as possible to its earlier condition of unrepaired damage. X-ray inspection for the detection of fatigue cracks under repair patches was found to be helpful, but not always conclusive.

Initially the elastomeric surface coating was removed only in local regions believed to be fatigue sensitive. For Specimens #7, #10, #11, #12, #13, and #14, the entire tension surface of the wing was stripped to permit unrestricted observation of crack propagation during testing. Cracks as small as 0.1 inch length could be detected without difficulty by visual inspection of critical regions of the stripped surface; prior knowledge of probable crack-prone locations was found to be highly important in the prompt detection of these small fatigue cracks. All initial crack lengths and their locations were tabulated prior to the start of testing.

Static residual strength testing was conducted by loading the specimen in successive increments of 10 percent Limit Load until a major failure occurred across the wing

cross section tension surface. Loading was stopped whenever any appreciable sonic reports were heard, the load was reduced to 20 percent Limit Load for safety during inspection, crack growths were measured and recorded, then testing was resumed. Normally the sonic reports associated with crack growth during static loading were sharp and distinct, and the associated crack propagation was often several inches in length.

Fatigue test cycling was conducted at a rate ranging from two to four cycles per minute, depending on load level, and was determined by the dynamic response of the loading system. Crack propagation data were recorded at intervals of 500 cycles or less, or whenever any sonic reports indicating crack propagation occurred. Progress of crack propagation was marked on the test specimens to provide visual records, and photographs were made of many of these locations.

After completion of 20,000 cycles of fatigue testing (or less if crack propagation damage was so extensive as to risk failure if fatigue testing were continued), a static residual strength test was conducted by the same procedure used for the test specimens which were not subjected to fatigue test cycling.

TEST RESULTS

Propagation behavior of the largest cracks is summarized in Table 3 for upbending tests and in Table 4 for downbending tests. The initial crack length, crack growth after cycling, and the final crack length at failure are noted. Failure loads achieved during residual strength test are shown in Figure 8 for each test specimen. Notes used to describe crack length data throughout the report are listed in Table 5. The more important numerical data on extent and location of initial cracking, formation of new cracks, and crack propagation records are shown in Tables 6 through 15; a comprehensive crack history for all 14 test specimens is given in Reference 1.

Static Residual Strength Tests

Upbending

Specimens #1, #2, and #3 were tested to evaluate wing lower surface crack propagation characteristics under increasing levels of static load. Predominant initial damage from service fatigue on all three of these specimens was at W. S. 176, near the termination of the spanwise reinforcing beam (see Figure 4). Their residual strength failure loads fell within a narrow range of 114 percent to 116 percent Limit Load at W. S. 176. Crack history is shown in Table 6.

Test Specimen #1. Test failure is shown in Figure 9. Close-up of failure in Figure 10 shows lower surface cross-section details, including hat section stringers. Several regions of the upper surface experienced compression-type secondary failures.

Test Specimen #2. Initial damage at W. S. 176L is shown in Figure 11. Test failure at this station appears in Figure 12. Secondary upper surface compression damage was extensive on this specimen, also.

Test Specimen #3. Initial damage at W. S. 176R in region of subsequent specimen failure is shown in Figures 13 and 14. Both cracks originated in the double row of fasteners attaching the reinforcing beam to the skin. This location is in the vicinity of the aft end of the engine thrust attachment angle.

The four initial cracks at the corners of the W. S. 120.5 door cutouts did not propagate.

Downbending

Specimens #6, #7, and #8 were tested to evaluate wing upper surface crack propagation characteristics under increasing levels of static load. Crack history for these specimens appear in Table 7.

Test Specimen #6. A view of cracks at W. S. 34.5L through the end fasteners of the reinforcing doubler is shown in Figure 15. The lighter region on the specimen is caused by removal of the elastomeric coating from the surface in the vicinity of initial damage; darker regions around the edges show where the coating remains. Note that the crack labeled Item 2, which propagated when loading was increased from 70 percent to 80 percent Limit Load, was arrested by the panel splice at its forward terminal and a fastener hole at its aft terminal. In Figure 16, the crack labeled Item 6 propagated from the edge of the W. S. 120.5 fuel filler plate past the fastener hole at 80 percent Limit Load, then jumped to the edge of the panel splice at 90 percent. This was the most crack growth observed on any test specimen at this location, although significant initial damage here was found on several test specimens. Primary failure occurred at 66 percent Limit Load (Condition D-1, Table 1) due to stripping of all barrel nut threads in the tension surface connections at the W. S. 220 joint. Extensive secondary failures occurred in the nearby box surface and beam structure which prevented the replacement of barrel nuts and continuation of the test.

Test Specimen #7. This was the only C-130B model tested; all others were C-130E models. Corrosion occurred during service, particularly in the panels adjoining the front and rear beam caps, but this had no evident relationship to the initiation or propagation of fatigue cracking.

Figure 17 shows the small cracks which had formed at the fuel filler opening. Both cracks were arrested by fastener holes.

A close-up view of the failure at W. S. 135R is shown in Figure 18. Initial crack lengths are indicated by Items 7, 8, and 9. These cracks initiated and propagated through the end fastener holes of the underlying reinforcement doubler. The "fingers" of the doubler may be seen protruding past the skin fracture surface. This type of failure (through end row of fastener holes) was observed repeatedly during the test program. As may be observed in Table 7, this was not the location of maximum initial cracking, which was at W. S. 105L.

Test Specimen #8. Principal initial damage was at the corners of the door cutout in the vicinity of W. S. 182 and W. S. 200, is illustrated in Figures 19, 20 and 21. Note that all of these cracks had one terminal at the edge of a cutout and the other terminal at a fastener or stopdrilled hole. As shown in Table 7, none of these cracks propagated appreciably.

Failure occurred at 117 percent Limit Load at W. S. 61R; no prior cracks had been reported or observed at this location. Cracking during test cycling was not observed at this location because the elastomeric coating had not been removed. Post-failure examination of the fracture surfaces revealed several small fatigue cracks under the heads of countersunk fasteners. Effective lengths of small cracks extending on both sides of countersunk fastener holes were sufficiently large to propagate catastrophically in the 7178 T-6 material at the stress levels associated with 117 percent Limit Load, particularly when stress concentration effects around fastener holes are considered. A similar type failure occurred during test #10 at W. S. 61L. However, the elastomeric coating had been removed and cracks were monitored visually during the test.

On all subsequent tests (Specimens #10, #11, #12, #13, and #14) the elastomeric coating was stripped from the entire tension surface to permit comprehensive visual inspection for cracks originating at any point, whether cracking was present initially or originated during fatigue test cycling or static residual strength testing.

Cyclic Crack Propagation Test

In a number of tests the largest initial cracks did not propagate appreciably, while cracks which were initially small - or even non-existent so far as could be observed - began to grow during cyclic testing to the extent that they eventually became the source of specimen failure. This behavior appeared to be substantially influenced by the extent of local redistribution of stress into reinforcing structure and/or encounter with a crack-arresting design feature.

Upbending

Specimens #4, #5, #13, and #14 were tested at a maximum of 10,000 cycles at each of two load levels to investigate the cyclic crack propagation behavior of the lower surface. Crack history for these specimens appears in Tables #8, #9, #10, and #11. After the completion of cyclic testing, the same loading condition was applied for the residual strength test.

Test Specimen #4. Initial damage was at the ends of the reinforcing beams (W. S. 176) and doubler (W. S. 168) extending past the W. S. 120.5 door cutout, generally through the holes for end fasteners attaching the reinforcement to the skin. After 7449 test cycles at 50 percent Limit Load, extent of cracking (see Table 8) was enough to warrant reduction of cyclic load level to 40 percent Limit Load. After 3400 cycles at this level, cyclic testing was halted because damage was considered sufficiently extensive to risk an uncontrolled failure of the specimen. Static residual strength testing was conducted with failure occurring at 64 percent Limit Load along an irregular line between W. S. 176L and W. S. 168L. An overall view of the failure is shown in Figure 22, while Figure 23 shows a close-up view of the failure; cracks 13 and 19 are across the end pair of fasteners attaching the reinforcing beam to the skin.

Test Specimen #5. A 1.1 inch crack at the corner of the door cutout at W. S. 113R was the only initial damage detected, and as shown in Figure 24 (Item 1), it propagated to only 4 inches during the entire test, and was not associated with eventual specimen failure.

Initial cyclic load level was 50 percent Limit Load. After 7000 cycles, a broken node was discovered on the left wing lower surface "rainbow fitting". These are large and complex fittings (extruded and machined) on both upper and lower wing surfaces which extend for the full length of the wing box chord at W. S. 220, and transfer primary surface loads across this main wing production joint (Figures 13, 25 and 26). At 7821 cycles, sonic reports were heard which led to discovery of three additional broken rainbow fitting nodes at Stringers #12, #16, and #17 on the opposite wing at W.S. 220R.

Cyclic load level was immediately reduced to 30 percent Limit Load, and cycling resumed to reach a total of 20,000 cycles. No further rainbow fitting node damage was observed during cyclic testing. Several fatigue cracks developed through the end row of fastener holes attaching the skin to the reinforcing doubler at W. S. 168L as shown in Figure 27 (Items 12, 13, and 14); note also in this figure the progression of the crack length at 60 percent, 70 percent and 80 percent Limit Load during subsequent static residual strength testing, and the crack arrest at the aft panel splice.

In the static residual strength test, four more nodes at the right wing rainbow fitting failed at 80 percent Limit Load, followed by total failure here at 87 percent (Figure 26).

Crack propagation records are shown in Table 9.

Test Specimen #13. This specimen was taken from a commercial airplane, and had approximately 13,000 flight hours and extensive repairs. The large patches in the vicinity of W. S. 58L and 58R were X-rayed to locate underlying cracks. X-ray examination confirmed field reports of a 9.4 inch skin crack in the center panel at W. S. 58L; most of these two large repair patches were removed as shown in Figures 28 and 29.

Crack growth records are shown in Table 10, and the progression of crack propagation at W. S. 59L is shown in Figure 30. The initial 9.4 inch crack terminated at a fastener hole and at the edge of a panel. Another initial crack of 3.4 inches existed at the same wing station in Panel #1; both ends terminated in holes. Slowness of these two cracks to grow is attributed to the inhibiting effect of the terminals being in fastener holes or at panel edges. The two hat stringers in the forward region of Panel #2 under the large crack were found to be partially cracked at 19,000 cycles.

This specimen showed some unexpected characteristics. Detectable sonic reports and subsequent measurements of appreciable crack propagation occurred at 42.7 percent, 44.4 percent and 52.3 percent Limit Load, as marked on Figures 28, 29, and 30. At this point approximately two-thirds of the central panel and one-third of the forward

panel were cracked (out of a total of three lower surface panels), and at least two hat section stringers were cracked. At 62.3 percent Limit Load, a very large sonic report was heard. Subsequent inspection disclosed that all of the forward and center panels and the reinforcing structure under these two panels were severed at W. S. 58L. However, the aft panel and both the front and rear spars appeared to be completely intact, and it was decided to continue the test. At 20 percent Limit Load, there was a 1/4 to 1/2 inch surface separation along the main crack at panels #1 and #2. At 53 percent Limit Load panel #3 failed. The subsequent inspection showed that the entire lower surface (all three panels) had completely failed. The spar caps were still intact, and held the severed edges of the failed panels together, with little separation along the failure line. The maximum residual strength is recorded as 62.3 percent Limit Load, the Load level reached prior to the failure of the center and forward panels.

Test Specimen #14. This specimen was taken from a commercial airplane, and it also had approximately 13,000 flight hours and extensive repairs. X-ray examination of reported cracks under repair patches revealed a 5.3 inch crack at W. S. 58R; most of two large patches were removed to permit crack propagation along this station without inhibition by repair patches. As shown in Figure 31, terminals of this 5.3 inch crack were at the edge of a panel and in a fastener hole. A total of 30 cracks were identified and recorded at the start of testing. Crack propagation records are shown in Table 11.

After 6297 cycles at 45 percent Limit Load, sonic reports were heard and the cycling halted for inspection. The cracks at W. S. 179R (marked in Figures 32 and 33) were partially visible externally (above patch in Figure 33) at 6022 cycles, and at 6297 cycles had reached a length of approximately 32 inches (most of which was externally obscured by the engine thrust attachment angle). Internal inspection disclosed the full extent of the skin crack and that hat stringers #15, #16, #17, and #18 were broken at this location. The cyclic load level was halved to 22.5 percent Limit Load to reduce the rate of cyclic damage and to avoid risk of an uncontrolled failure. During the 10,000 additional cycles at 22.5 percent Limit Load, another 20 cracks were initiated, but none of the larger cracks propagated appreciably.

Static failure occurred at 59 percent Limit Load at W. S. 179R. Examination of the failed surfaces disclosed an aged crack in a blind region between the external engine thrust angle and Stringer #16. This initial crack extended approximately 6 inches aft into Panel #2 and 1 inch forward into Panel #1. It was located immediately to the right of the repair patch over Stringer #16, as shown in Figure 34.

The largest initial crack detected, 5.3 inches at W. S. 58R (Figure 31), grew to 5.9 inches, terminating in the next fastener hole after 4500 cycles. This lack of propagation was surprising in view of the large initial crack length and the removal (prior to testing) of two large steel patches over the crack to permit unrestrained propagation.

Downbending

Specimens #9, #10, #11 and #12 were tested at a maximum of 10,000 cycles at each of two load levels to investigate the cyclic crack propagation behavior of the upper surface. Crack history for these specimens appears in Tables 12, 13, 14, and 15. At the completion of cyclic testing, a residual static strength test to destruction was conducted with test load condition D-2.

Test Specimen #9. 10,000 cycles at 25 percent Limit Load were applied, followed by 10,000 cycles at 22.5 percent Limit Load. Several considerations guided the selection of the 25 percent load. Elementary fracture mechanics analysis (see Table 2) indicated a cyclic load value in the 25 percent to 30 percent range and upbending crack propagation test of Specimens #4 and #5 had resulted in extensive damage from cyclic testing at 50 percent Limit Load. Also, the Al 7178 material in the upper surface had a lower fracture toughness than the Al 7075 T-6 of the lower surface. Thus, the initial cyclic load for Specimen #9 was set at 25 percent Limit Load, which was the smallest initial cyclic load used.

All initial cracks (Table 12) terminated at fastener or stopdrilled holes except one end of a 3.6 inch crack (W. S. 34.5L) which terminated under the flange of a reinforced hat section (Figure 35).

Significant crack growth data were recorded (Table 12) during the static residual strength test after sonic reports at 70 percent, 74 percent, 78 percent and 81 percent (failure) Limit Load. A view of the failure is shown in Figure 36. Note that the crack in the two forward panels passes through the fasteners at the outboard end of the "fingers" of the reinforcing doubler around the door cutout.

Test Specimen #10. 10,000 cycles each at 40 percent Limit Load and 35 percent Limit Load were applied. All three of the reported initial cracks were located in the corners of the W. S. 182.5-198.5 cutout, and all had one terminal at the edge of the cutout and the other at either a stopdrilled or a fastener hole, as shown in Figures 37, 38, and 39. The crack-stopping effectiveness of the panel edge splice is again demonstrated with the arrest of the large crack (Item 7) inboard and aft of the cutout (Figure 38). The elastomeric coating was completely stripped from the tension surface, permitting visual detection and monitoring of 12 new cracks that initiated at W. S. 61L during cyclic testing. These cracks initiated at fastener holes, as shown in Figures 40 and 41. Most of the cracking occurred after 18,000 cycles as shown in Table 13.

During static testing a loud sonic report was heard at 76 percent Limit Load. A 13.7 inch crack was found at W. S. 165R. There was no prior indication of cracking at this location. The crack-arrest effectiveness of the panel edge splices should again be noted (Figure 42), where additional propagation to the other edge of the panel occurred during subsequent testing at 88 percent Limit Load. Loading was reduced for inspection of crack growth associated with the sonic report at 88 percent Limit Load; when loading was resumed total chordwise failure occurred at W. S. 61L at 87 percent Limit Load, which was 1 percent lower than had been obtained on the preceding load application. The failure is shown in Figure 43, and is the culmination of the initial cracking shown in Figures 40 and 41.

Specimen #10 failed at the same station (opposite wing) as Specimen #8. Even though the elastomeric coating was stripped from the tension surface of Specimen #10, no initial damage was found at this location. Most of the cracks at W. S. 61L that developed and propagated during cyclic testing were so small it is unlikely they would have been detected if the elastomeric coating had not been removed. In contrast, the failure

location on Test Specimen #8 had been covered entirely by elastomeric coating, and inspection of the fracture surfaces (after failure at 117 percent Limit Load) revealed the prior existence of some small fatigue cracks around countersunk fastener holes. Thus, failures of Specimens #8 and #10 were similar, even though Specimen #8 had not been subjected to test cycling.

Test Specimen #11. Large areas of the wing upper surface were covered with repair patches. The wing box was examined visually and by X-ray to determine which patches should be removed. Cracks were found in the corners of the W. S. 183-199 door cutouts. These patches were removed to permit uninhibited growth of the cracks in the corners of the cutouts (Figure 45).

50 percent Limit Load was applied for 10,000 cycles and followed by 40 percent Limit Load for another 4500 cycles. Most severe fatigue damage occurred along the end row of fasteners at W. S. 213.5R (Figure 46). After 14,500 cycles, the only structure remaining intact in the aft region of the wing surface was the beam cap and fitting. Substantial skin cracking also occurred at the corresponding location on the opposite wing. Cycling was halted, and a static residual strength test conducted. Crack growth records are given in Table 14.

Initial cracks at the corners of the W. S. 183-199 door cutouts did not propagate extensively, even though one of these cracks was 4.1 inches long (terminated at stopdrilled hole - Figure 44). Similar behavior was observed for Specimen #10. Corrosion damage was observed, but was not sufficient to cause any loss of strength.

Test Specimen #12. Initial cracks on Specimen #12 were smaller than those on most of the other specimens. There was no obvious corrosion, and no major service repairs or reinforcements were installed. The initial cyclic load level was 50 percent Limit Load. After a few thousand cycles severe cracking occurred in several locations (Table 15). Damage at the eventual failure location appears in Figures 47 and 48. The hat sections in this area failed after a few thousand additional cycles because of the amount of load transferred to them from the cracked skin. An interior view of these broken hat sections

at W.S. 105L is shown in Figures 49 and 50. The progression of damage to failure is shown in Figure 51. Immediately prior to failure during the static test, a continuous skin crack extended over both panels #2 and #3 and across approximately 80 percent of panel #1 (out of a total of four panels), and six hat sections were broken under panels #2 and #3. Failure occurred at 56 percent Limit Load at W.S. 105L.

The extensive damage in Specimen #12 is attributed to the high cyclic loads (50 percent, then 40 percent Limit Load) and the absence of extensive fatigue-preventive repairs.

CONCLUSIONS

Crack propagation during static residual strength tests of the six specimens not subjected to test cycling generally was localized along one or two stations on each specimen; critical locations varied according to the prior flight history of each specimen. There was no consistent correlation between service-imposed fatigue damage and static residual strength.

For the eight specimens subjected to fatigue cycling prior to static residual strength testing, crack initiation and propagation tended to occur at many different locations. Fatigue cracks usually occurred in the vicinity of major structural discontinuities, such as termination of fastener patterns attaching reinforcing doublers and stiffeners to the skin, wing rib to surface attachments, access door cutouts, fuel filler openings, and drain holes. Cracks which initiated at the terminal fasteners attaching reinforcing doublers and stiffeners to the skin were prevalent.

The size and location of initial damage did not necessarily influence subsequent cyclic crack propagation or residual static strength behavior. None of the cracks which had been initiated during service or during the tests at the corners of cutouts propagated appreciably or were at the locations of eventual static failure, even though some of these cracks were four inches in length. This behavior is attributed to design features such as reinforcing structure, panel splices, and stopdrilled or fastener holes that arrest crack growth and permit redistribution of stresses in the vicinity of a crack terminal.

Direct application of elementary plate fracture mechanics theory was not a suitable means of predicting crack growth. The presence of reinforcing structure, uncertain stress distribution due to locally complex structural detail, crack tips in holes, and non-idealized boundary conditions and load distributions are significant features which are not accounted for in that theory.

The fatigue test cycling on the eight crack propagation specimens was generally much more severe in terms of equivalent fatigue damage, than the service-imposed damage which they had experienced. Extensive cracking occurred during cyclic testing in most of the specimens; in some instances more than half of the cross-sectional area of the tension surface was cracked. For the heavily damaged specimens, there was an approximate correlation between the amount of damage present at the end of cyclic testing and residual static strength. Damage tolerant structural design features, notably multi-element construction in the form of multiple spanwise wing panels and reinforcing hat stringers, were observed to be consistently effective in arresting crack growth; this was the predominant reason for the substantial residual strength capability demonstrated by these wings after extensive fatigue cracking had occurred.

The following static residual strength test levels were achieved for the directions of loading and prior fatigue experience as described.

- (1) Upbending, three specimens tested as received with service-imposed fatigue damage: 114 percent to 116 percent Limit Load. Maximum initial crack length on each specimen was 3.7 inches, 3.7 inches, and 2.0 inches, respectively. All of these cracks were located along the line of eventual wing failure.
- (2) Downbending, three specimens tested as received with service-imposed fatigue damage: 98 percent to 116 percent Limit Load. Maximum initial crack length on each specimen was 4.4 inches, 2.3 inches, and 1.2 inches, respectively. None of these cracks were located along the lines of eventual wing failures.

- (3) Upbending, four specimens tested as received with service-imposed damage and followed by cyclic testing prior to static test: 59 percent to 86 percent Limit Load. Maximum initial crack length on test specimen was 2.6 inches, 1.1 inches, 9.4 inches, and 5.3 inches. Wing failure subsequently occurred through the 2.6 inch and 9.4 inch cracks, but not through the 1.1 inch and 5.3 inch cracks. Post-failure examination of the specimen which did not fail through the 5.3 inch crack (W. S. 59R) revealed an aged crack of approximately 6 inches length had existed in a blind region between an internal hat section stringer and an external engine thrust angle; failure occurred at W. S. 179R.
- (4) Downbending, four specimens tested as received with service-imposed damage and followed by cyclic testing prior to static test: 56 percent to 81 percent Limit Load. Maximum initial crack length on each specimen was 3.6 inches, 1.5 inches, and 0.5 inches. Wing failures subsequently occurred through the 3.6 inch crack, but not through any of the others.

The greatest asset in crack detection was found to be a prior knowledge of fatigue-prone locations, which suggests the importance of prompt dissemination of information on the discovery of cracks to all operators of that model aircraft. Detection of cracks covered by the thick elastomeric surface coating was difficult, but after the coating was stripped from the surface, experienced inspectors consistently detected (by visual inspection) cracks as small as 0.1 inch in length. X-ray examination was helpful in detecting cracks in blind areas, but was not always reliable.

Reference

1. Reeder, Franklin L., Dirkin, William, and Snider, H. Lawrence: Results of C-130 Center Wing Residual Strength and Crack Propagation Test Program, NASA CR 112008, October, 1971.

APPENDIX

Beam runout: End of a reinforcing beam used to stiffen the lower surface access door cutout; there are two beams forward and two beams aft of each cutout. Inboard location is W. S. 58; outboard location is W. S. 176-182.

Initial damage: Service-imposed fatigue damage existing when the specimen was removed from the airplane for this test program.

Wing joint bolt node - One of the 13 upper surface or 15 lower surface center wing to outer wing main attachment bolt locations (W. S. 220).

Rainbow fitting - W. S. 220 upper or lower surface joint fitting which mates with the center wing and receives loads from the outer wing.

SYMBOLS

c	one-half of crack length, inches
F.S.	fuselage station, inches
K_c	critical stress intensity factor, ksi $\sqrt{\text{in.}}$
L	left wing
L.L.	Limit Load, Lbs
R	right wing or stress ratio $\left(\frac{\sigma_{\text{min}}}{\sigma_{\text{max}}}\right)$
t	thickness, inches
W.S.	wing station, inches
X_p	chordwise location of applied loading at ends of test specimen, inches
σ	axial stress, lbs./in. ²
σ_u	axial stress at ultimate load, lbs/in. ²
~	test load cycles
$\text{\textcircled{C}}$	center line

TABLE 1
TEST LOADS @ 100% LIMIT LOAD

		WING STATION		
		0	61.6	220
Upbending	Moment	32,437,800 in.lbs.	32,437,800 in.lbs.	21,349,800 in.lbs.
	Shear	0	70,000 lbs.	70,000 lbs.
	X_p of Shear		37.34% chord F.S. 554.13	
Downbending (D-1)	Moment	-26,542,494 in.lbs.	-26,542,494 in.lbs.	-17,566,600 in.lbs.
	Shear	0	-56,666 lbs.	-56,666 lbs.
	X_p of Shear		40% chord F.S. 559.24	
Downbending (D-2)	Moment	-27,077,361 in.lbs.	-27,077,361 in.lbs.	-13,033,300 in.lbs.
	Shear	0	-88,662 lbs.	-88,662 lbs.
	X_p of Shear		37.40% chord F.S. 554.42	

TABLE 2
FRACTURE MECHANICS ANALYSIS TO SELECT INITIAL CYCLIC STRESS LEVELS

Theoretical stress level = $\sigma = (\frac{1}{2} Kc) / \sqrt{\pi c}$									
Wing Surface & Material	Test specimen number	Location of largest initial cracks, W. S.	σ_U , nominal stress at 150% limit load, psi	Half crack length, c, inches	σ , psi	% limit load = $\frac{\sigma}{\sigma_U} \times 1.5$, %	% limit load used in Phase 1 cycling	Crack length at end of Phase 2 cycling, inches	Crack length after residual strength test
Upper surface, Al 7178 T-651 Extrusion (t = .10), Kc = 43,000	9	34.5L	51,000	*3.6/2 = 1.8	9,000	(9,000/51,000)(1.5) = 26.5	25	3.6	Failure
	9	135R	49,000	*2.8/2 = 1.4	10,200	(10,200/49,000)(1.5) = 31.2	25	2.9	2.9
	10	200R	44,000	*2.68/2 = 1.34	10,500	(10,500/44,000)(1.5) = 35.8	40	2.68	2.68
	11	182.5L	44,000	*4.1/2 = 2.05	8,500	(8,500/44,000)(1.5) = 29	50	5.2	5.2
	12	184L	44,000	**1.1/2 = .55	16,500	(16,500/44,000)(1.5) = 56.1	50	1.1	1.1
Lower surface, Al 7075-T6 Extrusion (t = .125), Kc = 62,000	4	176L	56,300	2.6/2 = 1.3	15,500	(15,500/56,300)(1.5) = 41.6	50	6.8	Failure
	5	113R	54,500	1.1/2 = .55	23,000	(23,000/54,500)(1.5) = 63.4	50	4.0	5.5
	13	58L	55,700	*9.4/2 = 4.7	7,500	(7,500/55,700)(1.5) = 20.2	35	16.8	Failure
	14	58R	55,700	*5.3/2 = 2.65	10,600	(10,600/55,700)(1.5) = 28.5	45	5.9	5.9

* Crack terminates in hole or at edge of panel.

** Under door.

TABLE 3
SUMMARY OF FATIGUE DAMAGE, FAILURE LOADS AND FLIGHT HOURS FOR UPBENDING TEST SPECIMENS

Specimen No.	Flight Hours	Description of Area of Crack Origin	Crack No.	Wing Station, In.	Initial Crack Length, In.	Upbending, Phase 1 Cyclic Test, R = 0.1			Upbending, Phase 2 Cyclic Test, R = 0.1			* Length After Residual Strength Test, In.	% Limit Load at Failure		
						Cycles	Max. Load, % Limit Load	Crack Length, In.	Cycles	Max. Load, % Limit Load	Crack Length, In.				
1	5,920	Beam runout	1	176.5L	3.7							Failure line 1.7 1.7	115.7 ↓ 115.7		
		Door cutout corner	2	113R	0.3										
		Door cutout corner	4	113L	0.3										
2	4,020	Beam runout	1	176L	3.7							Failure line Failure line Failure line	114.5 ↑ 114.5		
		Beam runout	2		1.0										
		Beam runout	3	176L	0.8										
3	6,094	Beam runout	2	176R	2.0						Failure line 2.0	115.4 115.4			
		Door cutout corner	7	113R	2.0										
4	4,493	Beam runout	1	176L	2.6	7,450	50	6.1	3,400	40	6.8	Failure line Failure line Failure line	64.8 ↓ 64.8		
		Beam runout	2	182L	1.3			4.9			4.9				
		Door cutout corner	5	112.8R	0.3			3.2			3.2				
5	6,296	Door cutout corner	1	112.8R	1.1	8,033	50	3.7	11,967	30	4.0	5.5 Failure line	86.8 86.8		
		Wing joint bolt node	16,17	220R											
13	13,000	Beam runout	3	181L	2.4	10,000	35	3.5	10,000	32.5	4.9	5.2 1.4 1.8 1.6 Failure line Failure line	62.3 ↑ 62.3		
		Drain hole	6	179L	0.2			0.9			1.4				
		Drill hole	7	173.5L	0.6			0.8			1.7				
		Door cutout corner	13	113L	0.1			1.1			1.6				
		Beam runout	15	S8L	3.3			3.3			5.2				
		Beam runout	16	S8L	9.4			9.4			16.8				
14	13,000	Doubler runout	17	168L	1.4	6,297	45	22.7	10,000	22.5	22.7	23.7 5.9 Failure line	59 ↓ 59		
		Beam runout ¹	24	S9R	5.3									5.9	5.9
		Beam runout	27	179R	2.5									3.3	3.3

TABLE 4

SUMMARY OF FATIGUE DAMAGE, FAILURE LOADS AND FLIGHT HOURS FOR DOWNBENDING TEST SPECIMENS

Specimen No.	Flight Hours	Description of Area of Crack Origin	Crack No.	Wing Station, In.	Initial Crack Length, In.	Downbending 1, Phase 1 Cyclic Test, R = 0.1			Downbending 1, Phase 2 Cyclic Test, R = 0.1			* Length After Residual Strength Test, In.	% Limit Load at Failure
						Cycles	Max. Load, % Limit Load	Crack Length, In.	Cycles	Max. Load, % Limit Load	Crack Length, In.		
6	7,374	Doubler runout	1	34.5L	4.4							7.0	96.3 ↑ 96.3
		Doubler runout	2	34.5L	0.3							7.1	
		W.S. 220 joint	9	220R	-							Failure line	
7	5,617	Fuel filler cutout	1	120.5L	0.3							1.6	97.7 ↑ 9.6 ↑ 97.7
		Doubler runout	3	105.5L	2.3							9.6	
		Doubler runout	9	135.3R	1.4							Failure line	
		Fuel filler cutout	14	120.5R	-							1.7	
8	7,892	Door cutout corner	1	199.8L	1.2							1.2	116.6 ↑ 1.4 ↑ 116.6
		Door cutout corner	3	182.3R	1.4							1.4	
		W.S. 61 rib cap	4	61R	-							Failure line	
9	11,251	Doubler runout	1	34.5L	3.6	10,000	25	3.6	10,000	22.5	3.6	Failure line	81 ↑ 0.5 ↑ 19.8 ↑ 81
		Doubler runout	2	34.5L	0.5			0.5			0.7	Failure line	
		Doubler runout	3	37.5R	0.8			0.8			1.3	19.8	
		Doubler runout	4	135R	2.8			2.8			2.9	2.9	
10	6,603	W.S. 61 rib cap	6	61L	-	10,000	40	1.4	10,000	35	1.6	Failure line	87 ↑ 1.9 ↑ 1.4 ↑ 87
		Door cutout corner	2	182L	0.8			1.9			2.5	3.0	
		Door cutout corner	1	198.5L	0.8			1.1			1.3	1.4	
		Door cutout corner	3	199R	1.5			1.5			1.5	1.5	
11	7,660	W.S. 200 joint	9	213.5R	-	10,000	50	3.6	4,500	40	17.3	Failure line	57.3 ↑ 10.3 ↑ 57.3
		Fwd spar cap	3	178.5R	0.8			1.1	4,500		1.7	10.3	
		Door cutout corner	1	182.5L	3.0			4.0			4.1	4.1	
12	5,674	Doubler runout	3	105L	0.1	4,034	50	19.7	6,466	30	19.7	Failure line	56 ↑ 1.7 ↑ 1.6 ↑ 12.9 ↑ 1.6 ↑ 56
		Fuel filler cutout	1	120.5L	0.3			1.7			1.7	1.7	
		Fuel filler cutout	2	120.5L	0.3			1.6			1.6	1.6	
		Doubler runout	8	135L	0.5			12.9			12.9	12.9	
		Fuel filler cutout	9	120.5R	0.1			1.6			1.6	1.6	
		Fuel filler cutout	10	120.5R	0.3			4.2			4.2	4.2	

* Downbending 2 condition used for all specimens except Number 6.

TABLE 5

NOTES USED THROUGHOUT THE REPORT ON CRACK LENGTH DATA TABLES

- (a) All length measurements are given to the nearest 0.1 inch.
- (b) The crack terminated in edge of panel.
- (c) The crack terminated in fastener hole.
- (d) See Table 1 for loading conditions.
- (e) The crack terminated in stopdrilled hole.
- (f) A W.S. 220 rainbow fitting node cracked.
- (g) Stringers numbered 15, 16, 17 and 18 were also found to be broken.
- (h) The crack disappeared under an external repair.
- (i) This damage was discovered during an inspection after the residual strength test.
- (j) The crack appeared from the opposite side of an external repair.
- (k) On Specimen #13, at 19,000 cycles, stringers 17 and 18 were discovered to be partially broken, 17 from its aft flange to the centerline and stringer 18 from its fwd flange to its centerline.
- (l) On Specimen #12 broken stringers were found as follows: No. 5 after 2,870 cycles, No. 4 after 4,034 cycles, Nos. 3, 6, 7 and 8 after 10,500 cycles.

TABLE 6
MAJOR CRACK LENGTHS FOR LOWER SURFACE, STATIC UPBENDING TESTS

Test Specimen No.	Crack No.	Description	Wing Sta., Inches	Crack Location	Initial Crack Length, Inches	87% Limit Load	100% Limit Load	110% Limit Load	Failure Load	
1	1	The crack originated in the edge of holes common to the W.S. 120 cutout reinforcement beam and the skin.	176.5L	0.5" fwd & aft of the stringer 16 C	3.7(b)	3.7			Complete Chordwise Failure at 115.7% Limit Load	
	3	Same as crack 1	176.5L	0.5" fwd & aft of the stringer 20 C		7.0				
2	1	The crack originated in the edges of fasteners common to the W.S. 120 cutout reinforcement beam and the skin.	176L	0.5" fwd & aft of the stringer 16 C	3.7 ^(b) _(c)		5.0	5.0	Complete Chordwise Failure at 114.5% Limit Load	
	2	The crack originated in a drain hole in the skin.	176L	2.3" aft of the stringer 15 C	1.0(b)		1.0	1.0		
	3	Same as crack 1	176L	0.5" fwd & aft of the stringer 20 C	0.8		7.5(b)	9.5		
3	1	The crack originated in the edge of fastener holes common to the W.S. 120 cutout reinforcement beam and the skin.	176R	0.5" fwd & aft of the stringer 15 C	0.5		3.0		Complete Chordwise Failure at 115.4% Limit Load	
	2	Same as crack 1	176R	0.5" fwd & aft of the stringer 16 C	2.0		3.8			
	3	Same as crack 1	177R	0.5" fwd & aft of the stringer 20 C	0.1		0.1			
	4	Same as crack 1	176R	0.5" fwd & aft of the stringer 21 C	0.7		0.7			
	7	The crack originated in the edge of an access door attachment fastener hole.	113R	0.8" aft of the stringer 17 C	2.0 ^(b) _(c)		2.0			2.0
	10	Same as crack 1	176L	0.5" fwd & aft of the stringer 16 C	1.5		1.5			6.0 ^(b) _(c)

TABLE 7

MAJOR CRACK LENGTHS FOR UPPER SURFACE, STATIC DOWNBENDING TESTS

Test Specimen No.	Crack No.	Description	Wing Sta. In.	Crack Location	Initial Crack Length, Inches	After Applying 72.3% Limit Load	After Applying 77.8% Limit Load	After Applying 90% Limit Load	After Failure
6	1	The crack originated in the edge of a last fastener hole common to the internal reinforcing doubler of the access door cutout and the skin.	34.5L	The stringer 5 ☐	4.4			7.0	7.0
	2	Same as crack 1	34.5L	0.8" aft of the stringer 4 ☐	0.3			7.1	7.1
	6	The crack originated under the circular external repair doubler	120.5L	2.5" fwd of the stringer 6 ☐			0.5	4.1(b)	4.1
	8	Same as crack 1	37.5R	Same as 1				10.7(b)	10.7
	9	Barrel nuts attaching the specimen to the test frame were stripped resulting in specimen failure at the wing joint	220R	Rainbow fitting					Complete Chordwise Failure at 96.3% Limit Load.
7	2	The crack originated in the edge of the last fastener hole common to the internal reinforcing doubler of the fuel filler cutout.	105.5L	2.7" aft of the stringer 4 ☐	0.7				9.6(c)
	3	Same as crack 2	105.5L	2.7" fwd of the stringer 6 ☐	2.3			2.7	
	6	Same as crack 2	105.5R	2.7" fwd of the stringer 6 ☐	1.4(e)				1.9(c)
	7	Same as crack 2	135.3R	2.7" aft of the stringer 4 ☐	0.7				
	8	Same as crack 2	135.3R	0.8" aft of the stringer 5 ☐	0.5				
	9	Same as crack 2	135.3R	2.7" fwd of the stringer 6 ☐	1.4				
	10	Same as crack 2	135.3R	2.7" fwd of the stringer 5 ☐	0.1				Complete Chordwise Failure at 97.7% Limit Load.
8	1	The crack originated in the edge of a fastener hole. The hole, common to the door doubler and skin, was one of a row adjacent to the access door attachment fasteners.	199.8L	0.5" fwd of the stringer 5 ☐	1.2				1.2
	2	Same as crack 1	182.3L	0.5" aft of the stringer 2 ☐	0.7(e)				0.7
	3	Same as crack 1	182.3R	0.5" aft of the stringer 2 ☐	1.4				1.4
	4	Cracks originated in the edges of fastener holes common to the skin and the rib	61R	From front to rear beam along the W.S. 61R rib cap					Complete Chordwise Failure at 116.6% Limit Load.

TABLE 8

MAJOR CRACK LENGTHS FOR LOWER SURFACE, CYCLIC UPBENDING TESTS - SPECIMEN NO. 4

Crack No.	Description	Wing Sta. In.	Crack Location	Upbending, Phase 1 Cyclic Test, R = 0.1 Max. Load = 50% Limit Load												Upbending, Phase 2 Cyclic Test, R = 0.1 Max. Load = 40% Limit Load						Length After Failure			
				Number of Cycles (d)												Cumulative Number of Cycles (d)									
				0	500	1000	1500	2000	2500	3000	3500	4000	4500	5000	5500	6000	6500	7000	7450	8000	8500		9000	9500	10,000
19	The crack originated in the edge of fastener holes common to the skin and the W.S. 120L door cutout reinforcement uen...	181L	0.5" fwd & aft of the stringer 15 ☐												2.3	3.2	3.2	3.5	4.0	4.3	4.9	5.8	6.9	Complete Chordwise Failure at 64.8% Limit Load	
13	Same as crack 19	180L	0.5" fwd & aft of the stringer 16 ☐							0.8	0.8	1.1	1.9	2.3	2.3	2.4	2.6	2.6	2.8	3.0	3.2				
1	Same as crack 19	176L	0.5" fwd & aft of the stringer 16 ☐	2.6	2.9(c)	2.9	2.9	3.7 ^(b) (c)	3.7	4.5	4.8	5.5	6.1(c)	6.1	6.3	6.7	6.8								
12	The crack originated in the edge of the last fastener hole common to the access door cutout doubler and the skin	168L	At the stringer 17 ☐							0.8	1.0	1.0	1.3	1.8	2.7	3.0	3.3(c)	3.9	4.2	4.9	9.5	14.5			
29	Same as crack 12	168L	At the stringer 18 ☐																	0.2	0.2				
27	Same as crack 12	168L	2.8" aft of the stringer 18 ☐																	2.7	3.2				
28	Same as crack 12	168L	At the stringer 19 ☐																	0.3	0.3	1.2			
14	The crack originated in the edge of a drain hole in the skin	175L	2.7" aft of the stringer 19 ☐							1.2	1.7	1.9(c)	2.2(c)	2.2											
2	Same as crack 19	182L	0.5" fwd & aft of the stringer 20 ☐	1.3	1.4	2.2	2.7	3.2(c)	3.8(b)	3.8	4.2	4.6	4.7	4.8	4.9(c)	4.9									
4	Same as crack 19	176L	0.5" fwd & aft of the stringer 21 ☐	0.6	0.9	1.6	2.1	2.5	3.0(c)	3.0	3.6	3.7	4.5	4.7	5.2	5.3	5.5	5.7	5.9	7.3					
9	Same as crack 19	176L	0.5" fwd & aft of the stringer 15 ☐			0.2	0.8	1.0	1.8	1.9	2.7	3.1	3.3(c)	3.5	3.7	3.8	4.2	4.2	4.9	5.7	6.0	6.2	6.3	6.4	6.6
6	Same as crack 19	176R	0.5" fwd & aft of the stringer 16 ☐	0.7	1.1	2.0	2.3	2.7(c)	3.1(c)	3.1	4.1(b)	4.1	4.5	4.7	5.2	5.7	5.9(c)	5.9	6.0	6.0					
7	The crack originated in the edge of a door attachment fastener hole	112.8L	0.8" fwd of the stringer 17 ☐	0.3(b)	0.3	1.0	1.3	1.5	1.6(c)	1.6	2.5	2.9	3.2(c)	3.2	3.7	4.3	4.9								

TABLE 10

MAJOR CRACK LENGTHS FOR LOWER SURFACE, CYCLIC UPBENDING TESTS - SPECIMEN NO. 13

Crack No.	Description	Wing Sta. In.	Location	Upbending, Phase 1 Cyclic Test, R = 0.1 Max. Load = 35% Limit Load								Upbending, Phase 2 Cyclic Test, R = 0.1 Max. Load = 32.5% Limit Load								Residual Strength Test											
				Number of Cycles (a)								Cumulative Number of Cycles (a)																			
				0	2000	3000	4000	5000	6000	7000	8000	9000	11,000	12,000	13,000	14,600	15,000	18,000	18,500	19,000	19,500	20,000	42.7%	44.4%	52.3%	62.3%	53%				
40	The crack originated under an external "slingshot" doubler repair at the end of the internal reinforcing beam of the access door cutout	181.4L	2.0" aft of the stringer 15	0.6																				0.6	1.1						
3	The crack originated under an external "slingshot" doubler repair at the end of the internal reinforcing beam of the access door cutout	181L	2.0" aft of the stringer 16	2.4	2.6	2.8	3.0	3.2	3.4	3.4	3.5	3.5	3.7	3.8	3.8	4.1	4.2	4.6	4.7	4.8	4.8	4.9	4.9				5.2				
4	The crack originated in the edge of a fastener hole common to a stringer flange and the skin immediately adjacent to a repair	181L	1.8" fwd of the stringer 20	1.0	1.2	1.2	1.4	1.5	1.6 ^(c) _(a)	-----															1.6						
5	Same as 3 except the crack emerged from both sides of the repair doubler	180.4L	1.0" fwd & aft of the stringer 20	3.3	----- 3.3			3.4	----- 3.4		3.5	3.8	----- 3.9 ^(b)			-----					3.9										
7	The crack originated in the edge of a drain hole in the skin	173.5L	2.8" fwd of the stringer 18	0.6	----- 0.6		0.7	----- 0.7		0.8	----- 0.8		1.1	----- 1.1		1.3	1.5	----- 1.7			1.7	1.8									
20	The crack originated in the edge of fastener holes common to the internal reinforcing beam for the access door cutout and the skin near a repair	179.5R	0.5" fwd & aft of the stringer 21	3.4 ^(c)	-----															3.4	3.5	-----				3.5 ^(c)					
11	The crack originated at a door attachment fastener	128L	0.8" fwd of the stringer 17	1.6 ^(c) _(b)	-----																			1.6							
12	Same as crack 11	128L	0.8" aft of the stringer 19	1.6 ^(b) _(c)	-----																			1.6							
14	Same as crack 11	113L	0.8" aft of the stringer 19	1.6 ^(b) _(c)	-----																			1.6							
17	Same as crack 11	113R	0.8" fwd of the stringer 17	1.2 ^(b)	1.2	1.3	----- 1.3		1.4	1.5	----- 1.5			1.6 ^(c)	-----							1.6									
15	The crack originated in the last fastener holes inboard common to the reinforcement beam for the access door cutout and the skin	58L	0.5" fwd and aft of the stringer 15	3.3 ^(c)	-----															3.3	3.8	4.0	4.6	5.2 ^(b)	5.2	7.6	9.1 ^(c)	9.1	25.9 ^(b)		Complete Chordwise Failure
16	Same as crack 15	58L	0.5" fwd and aft of the stringer 16	9.4 ^(b) _(a)	-----								9.4	10.8	11.9	12.6	13.5 ^(c)	13.8	14.0	14.6 ^(k)	15.2	16.8	17.7	17.7	20.9	27.2					

TABLE 12

MAJOR CRACK LENGTHS FOR UPPER SURFACE, CYCLIC DOWNBENDING TEST - SPECIMEN NO. 9

Crack No.	Description	Wing Sta. In.	Crack Location	Downbending 1, Phase 1 Cyclic Test, R = 0.1 Max. Load = 25% Limit Load				Downbending 1, Phase 2 Cyclic Test, R = 0.1 Max. Load = 22.5% Limit Load				Downbending 2 Residual Strength Test									
				Number of Cycles (d)				Cumulative Number of Cycles				70% Limit Load	74% Limit Load	78% Limit Load	81% Limit Load						
				0	4000	7500	8000	8500	13,000	14,000	17,000	19,000	19,500	20,000							
1	The crack originated in the edge of a last fastener hole common to the internal reinforcing doubler of the access door cutout and the skin	34.5L	The stringer 5 ☺	3.6				3.6				3.7		8.2	Complete Chordwise Failure						
2	Same as crack 1		0.5" fwd of the stringer 2 ☺	0.5(e)				0.5				0.7	3.9	10.4		10.6					
11	Same as crack 1		0.5" aft of the stringer 2 ☺	0.9(e)				0.9													
7	Same as crack 1		0.5" fwd of the stringer 3 ☺	0.1				0.1													
10	Same as crack 1	34.5L	0.5" fwd of the stringer 4 ☺										2.8(b)								
3	Same as crack 1	37.5R	0.5" fwd of the stringer 5 ☺	0.8				0.8				0.9	0.9	1.0		1.1	1.1	1.3	2.3	19.8(b)	19.8
4	The crack originated in the edge of a last fastener hole common to the internal reinforcing doubler of the fuel filler hole and the skin.	135R	2.8" fwd of the stringer 4 ☺	2.8(e)				2.8				2.9				2.9					

TABLE 13

MAJOR CRACK LENGTHS FOR UPPER SURFACE, CYCLIC DOWNBENDING TEST - SPECIMEN NO. 10

Crack No.	Description	Wing Sta. In.	Crack Location	Downbending 1, Phase 1 Cyclic Test, R = 0.1 Max. Load = 40% Limit Load							Downbending 1, Phase 2 Cyclic Test, R = 0.1 Max. Load = 35% Limit Load					Downbending 2 Residual Strength Test							
				Number of Cycles (d)							Cumulative Number of Cycles (d)					76% Limit Load	84% Limit Load	88% Limit Load	87% Limit Load				
				0	3000	3500	4000	4500	6000	7500	8000	9000	10,000	1,500	12,500					14,500	16,000	18,000	20,000
6	Originated in the edge of a fastener hole common to the skin and rib	61L	3.8" fwd of the stringer 1 ☐	1.1	-----					1.1	1.3	1.4	-----			1.4	1.5	1.5	1.6	1.6	2.1	2.1	Complete Chordwise Failure
19	Same as crack 6		2.7" aft of the stringer 1 ☐														1.0	1.0	2.4	2.4			
25	Same as crack 6		4" aft of the stringer 1 ☐															0.1		0.1			
24	Same as crack 6		2.7" aft of the stringer 2 ☐															0.2		0.2			
17	Originated in the edge of a fastener hole common to the skin and stringer flange		1.8" aft of the stringer 3 ☐															0.2	0.2	4.0			
18	Same as crack 17		1.8" fwd of the stringer 4 ☐															0.2	0.2	1.5	2.2		
20	Same as crack 6		4" aft of the stringer 4 ☐															0.5		0.5			
27	Same as crack 17		2.8" aft of the stringer 6 ☐															0.1		0.1			
23	Same as crack 6		2.7" fwd of the stringer 10 ☐															0.1		0.1			
22	Same as crack 6	61L	2.8" fwd of the stringer 11 ☐															0.3		0.3			
11	Same as crack 6	61L	3.8" aft of the stringer 11 ☐	0.3	-----					0.3	0.4	-----			0.4	0.5		0.5	9.9				
29	The crack originated in the edge of the first fastener hole beyond an external repair doubler	49.5L	1.8" aft of the stringer 5 ☐																	9.8	20.0		
7	The skin crack originated in the edge of one of the fastener holes in the row adjacent to the row of access door attachments.	174L	0.5" fwd of the stringer 5 ☐			0.9	1.0	1.1	1.3	1.4	1.5	1.7	1.9	2.1	2.3	3.1	3.5	3.8	5.1	10.5	10.5		
28	The skin crack originated in the edge of a fastener hole common to a stringer flange.	165.4R	1.8" fwd of the stringer 5 ☐															13.7	13.7	19.7	19.7		

35

TABLE 15
MAJOR CRACK LENGTHS FOR UPPER SURFACE,
CYCLIC DOWNBENDING TEST - SPECIMEN NO. 12

Crack No.	Description	Wing Sta. In.	Crack Location	Downbending 1, Phase 1 Cyclic Test, R = 0.1 Max. Load = 50% Limit Load							Downbending 1, Phase 2 Cyclic Test, R = 0.1 Max. Load = 30% Limit Load							Downbending 2 Residual Strength Test			
				Number of Cycles (d)							Cumulative Number of Cycles (d)							50%	53%	56%	
				0	500	1000	1500	2000	2500	3000	3500	4000	4500	5000	6500	7000	7036	9034	9500	10,000	10,500
32	The crack originated in the edge of a fastener hole common to the skin and stringer flange	107L	2.8" aft of the stringer 3 ζ															6.9 ^(b) 6.9 ^(c)	10.5	17.0	Complete Chordwise Failure
3	The crack originated in the edge of a fastener hole common to the skin and filler hole doubler runout	105L	2.8" fwd of the stringer 5 ζ	0.1	0.2	0.6	9.5	19.4 ^(b)	19.7								19.7 ⁽¹⁾	19.7			
18	Same as crack 3		0.5" fwd of the stringer 5 ζ		0.4	0.6															
6	Same as crack 3		0.5" aft of the stringer 5 ζ	0.1	0.6	0.9															
4	Same as crack 3		2.8" aft of the stringer 5 ζ	0.6	0.7	0.8	2.7														
5	Same as crack 3	105L	2.8" fwd of the stringer 6 ζ	0.6	0.8	0.9															
30	Same as crack 32	107L	2.8" aft of the stringer 6 ζ							2.6 ^(b) 2.6 ^(c)	2.6	3.0	6.3	9.1	12.6	12.6	19.1	19.1	19.9		
1	The crack originated in the edge of a fastener hole common to the fuel filler fitting and the skin	120.SL	2.5" fwd of the stringer 5 ζ	0.3	1.2	1.7 ^(b)											1.7	1.7			
2	Same as crack 1	120.SL	2.5" aft of the stringer 7 ζ	0.3 ^(c)	1.6 ^(c)												1.6	1.6			
26	Same as crack 3	135L	2.7" aft of the stringer 4 ζ			0.2	0.2														
7	Same as crack 3		2.8" fwd of the stringer 5 ζ	0.1		0.1	0.3														
19	Same as crack 3		0.5" fwd of the stringer 5 ζ		0.1	0.6	0.6														
8	Same as crack 3		0.7" aft of the stringer 5 ζ	0.5	0.5	0.8	1.0	1.3	6.5 ^(e)	6.5	9.5 ^(c)	12.9 ^(c)	12.9				12.9	12.9			
23	Same as crack 3	135L	2.8" fwd of the stringer 6 ζ			0.6															
10	Same as crack 1	120.SR	2.5" aft of the stringer 5 ζ	0.3 ^(c)	1.1	1.8	2.2	3.0	3.2	3.3	3.9	4.2					4.2	4.2			
11	Same as crack 3	109R	2.8" aft of the stringer 4 ζ		0.5	0.5	0.6	0.9	2.7	6.5	11.0	11.1					11.1	11.1			
15	Same as crack 3		2.8" fwd of the stringer 5 ζ		0.5	0.5	0.8	0.9	0.9												
20	Same as crack 3		0.5" fwd of the stringer 5 ζ			0.2	0.2	0.3													
12	Same as crack 3		0.5" aft of the stringer 5 ζ		0.6	0.6	0.9	1.1	1.8												
14	Same as crack 3	109R	2.8" fwd of the stringer 6 ζ		0.1	0.1	0.2	0.6	0.8	1.0											
16	The crack originated in the edge of a fastener hole common to the door doubler and skin	35R	0.5" fwd of the stringer 5 ζ		0.7	0.2	3.6	4.2	5.2	7.1 ^(c)							7.1	7.2			



Figure 1. - Used C-130 center wing boxes stored for testing

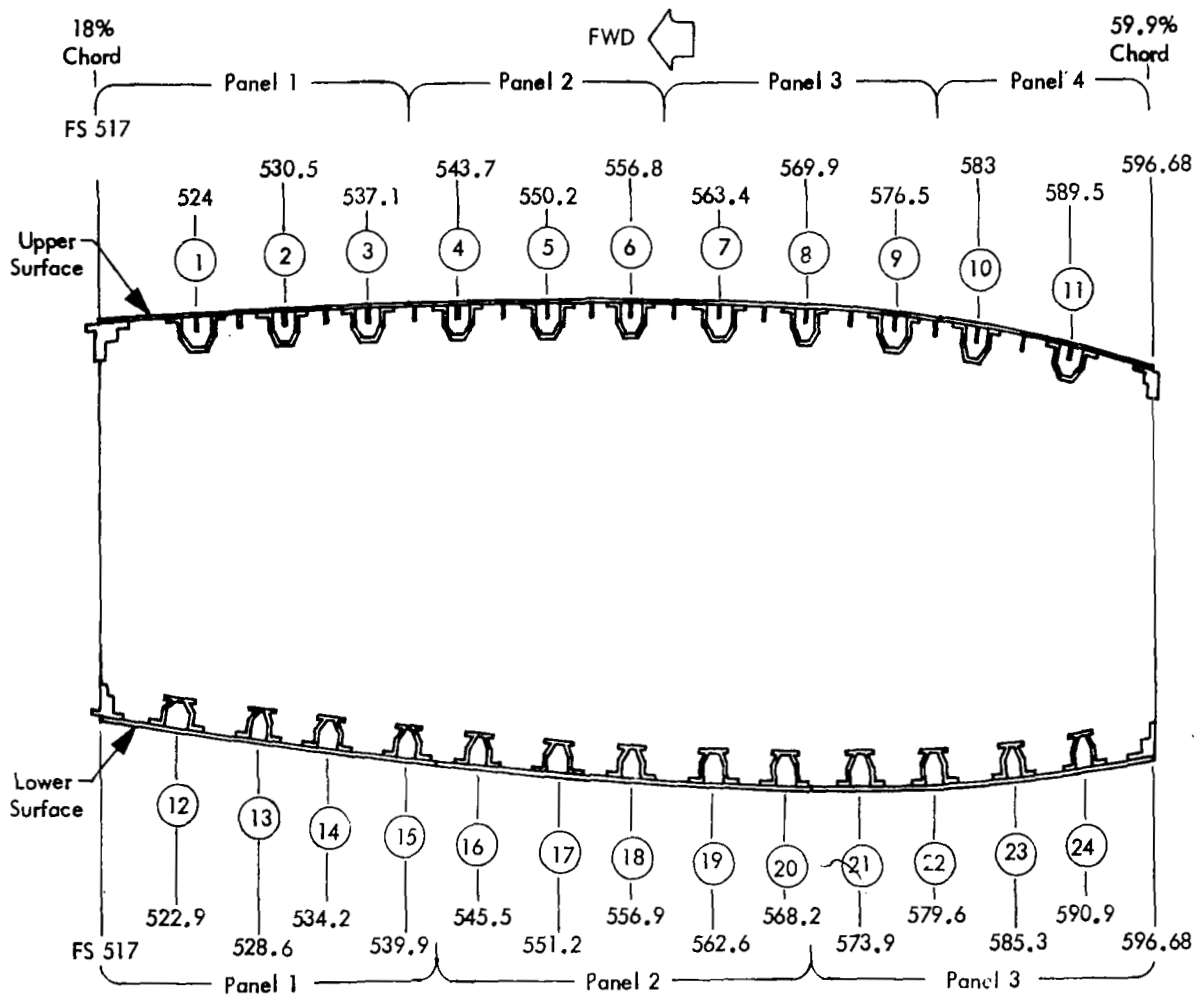


Figure 2. - General cross-section of center wing showing locations of stringers and skin panels.

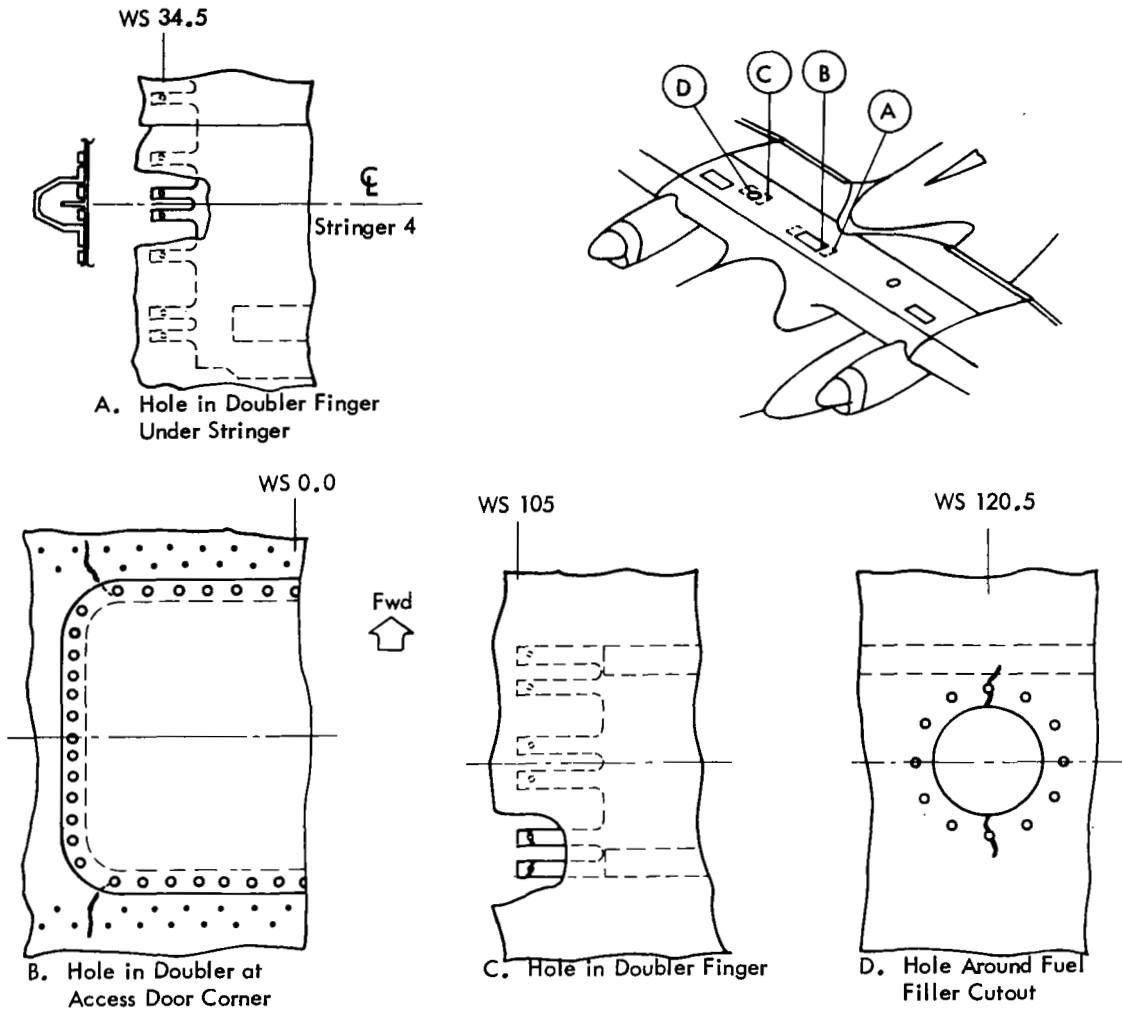


Figure 3. - Typical areas identifying upper surface skin cracks originating in fastener holes.

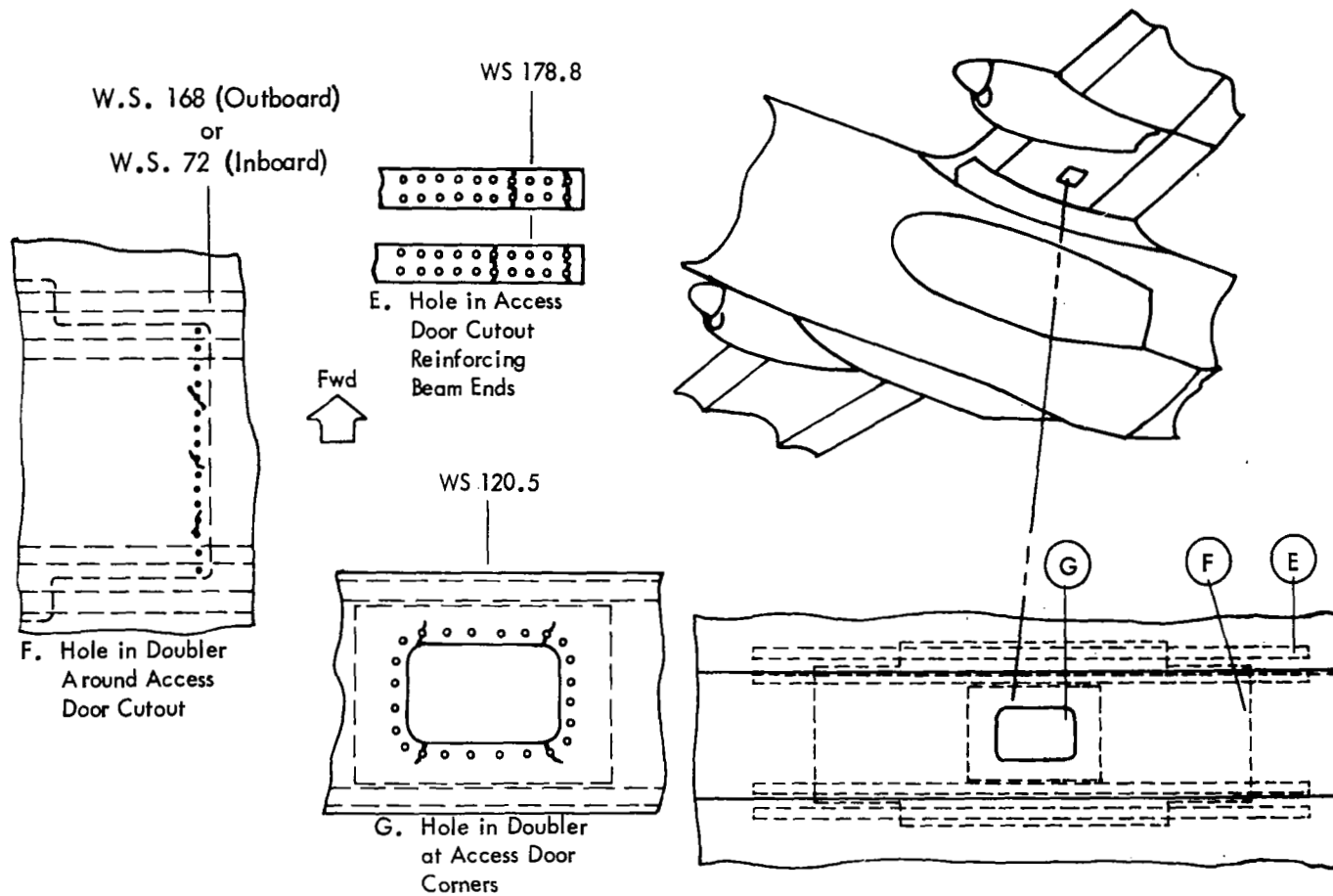


Figure 4. - Typical areas identifying lower surface skin cracks originated from fastener holes.

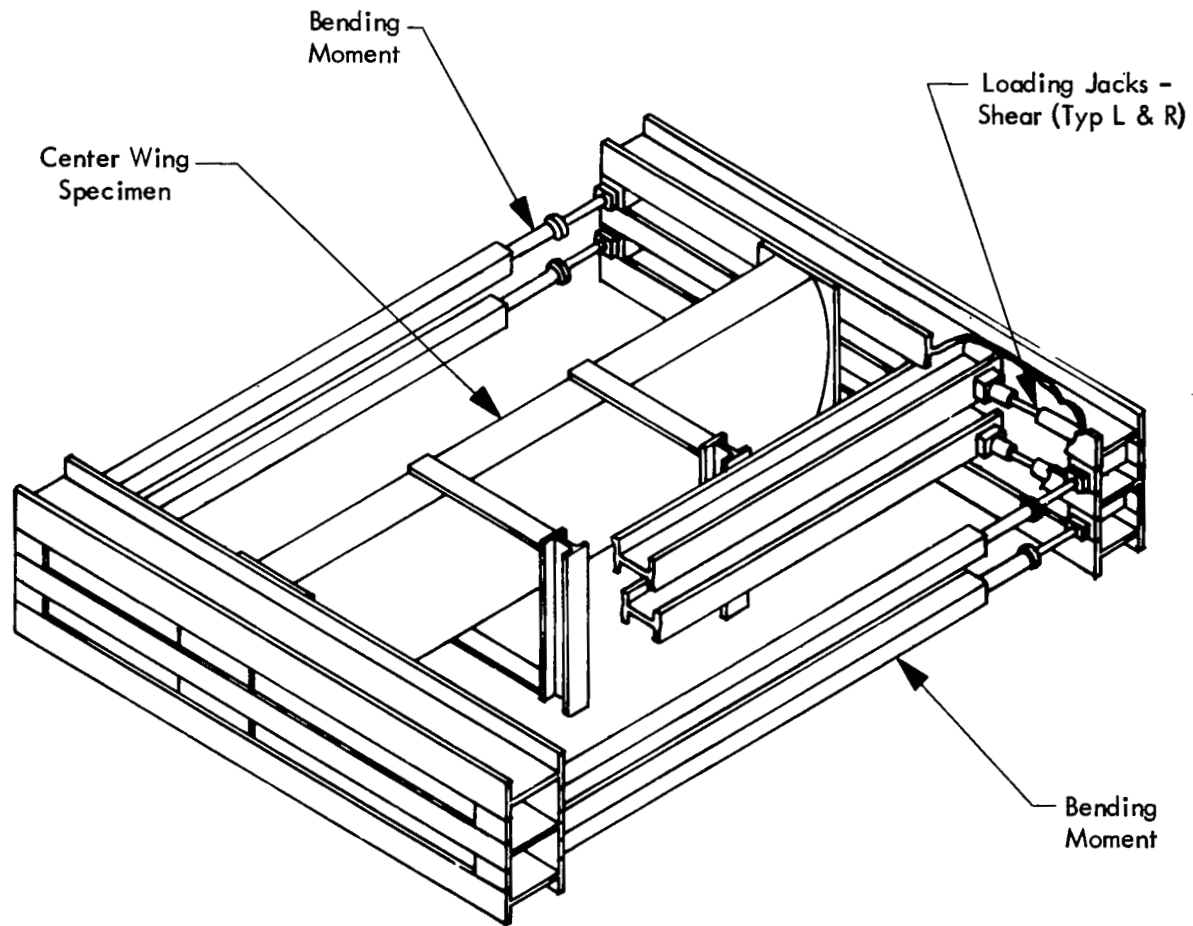


Figure 5. - Test loading fixture.

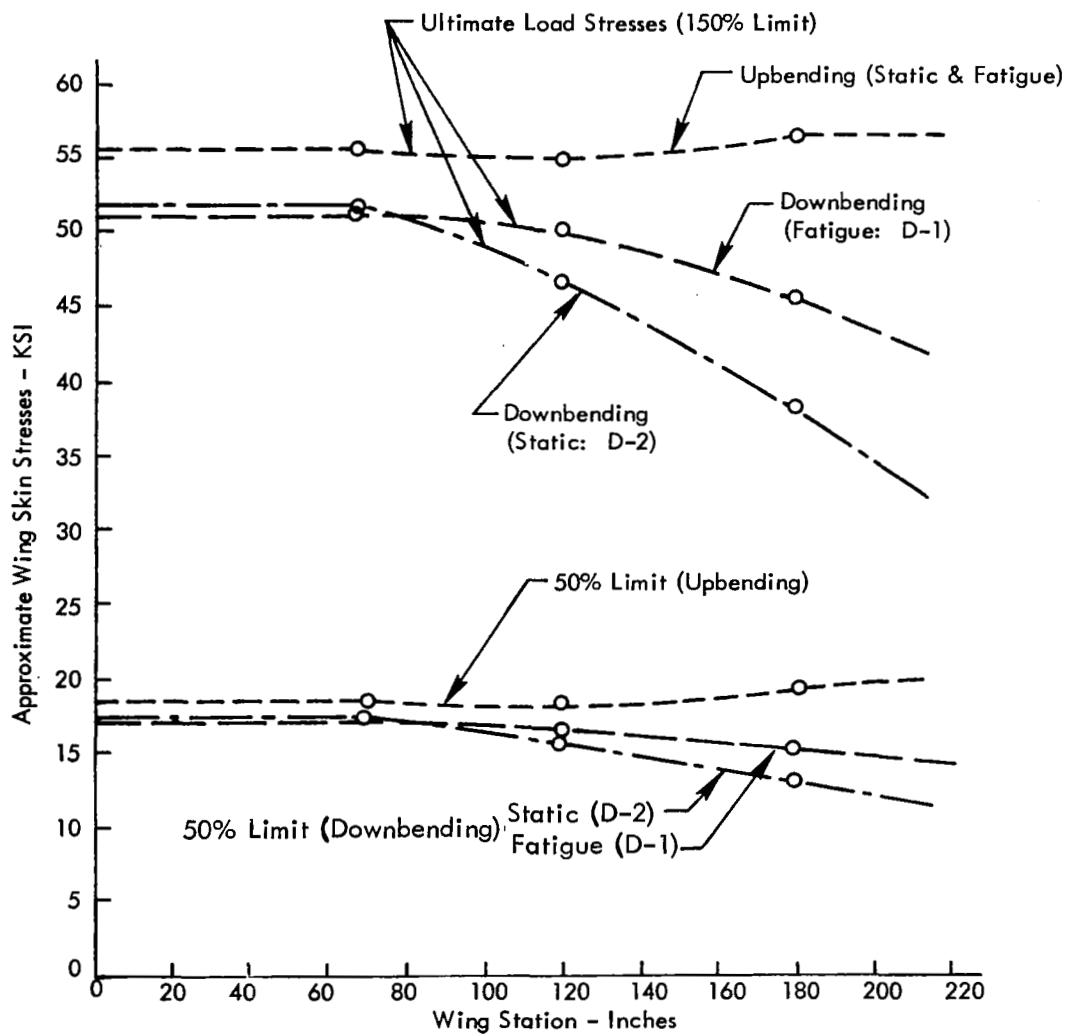


Figure 6. - Approximate wing skin stresses

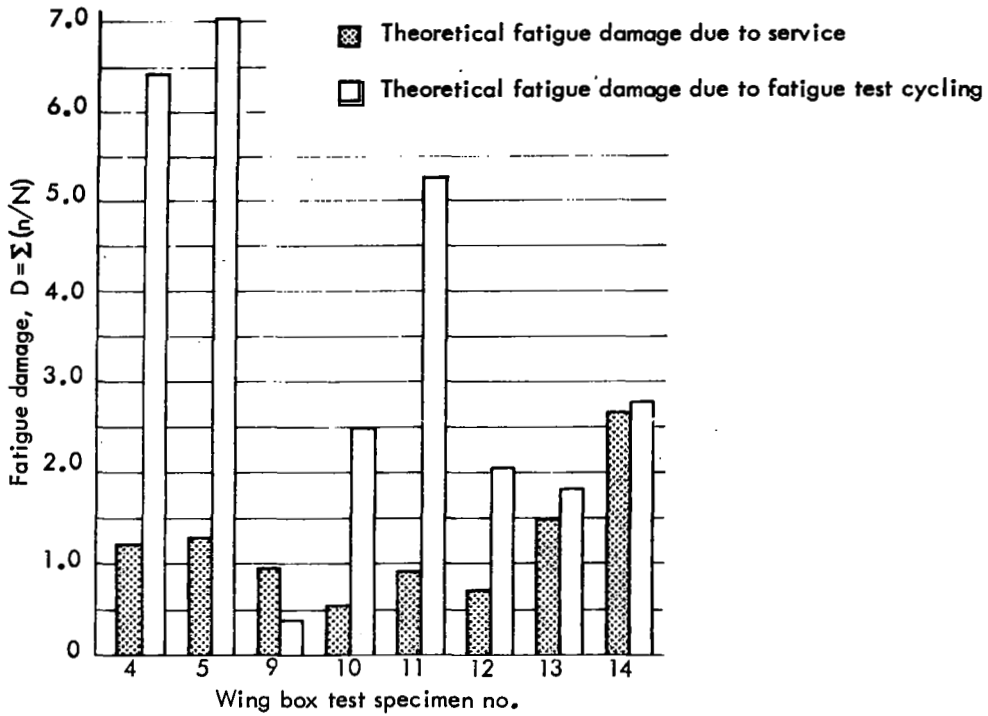


Figure 7. - Comparison of fatigue damage: service vs. test cycling

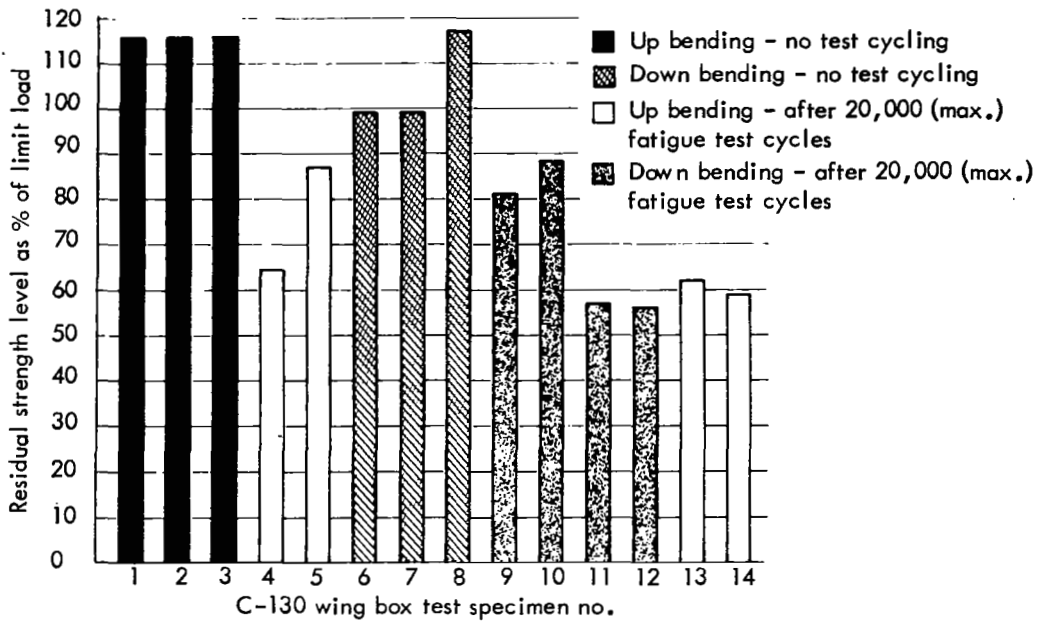


Figure 8. - C-130 wing box residual strength.

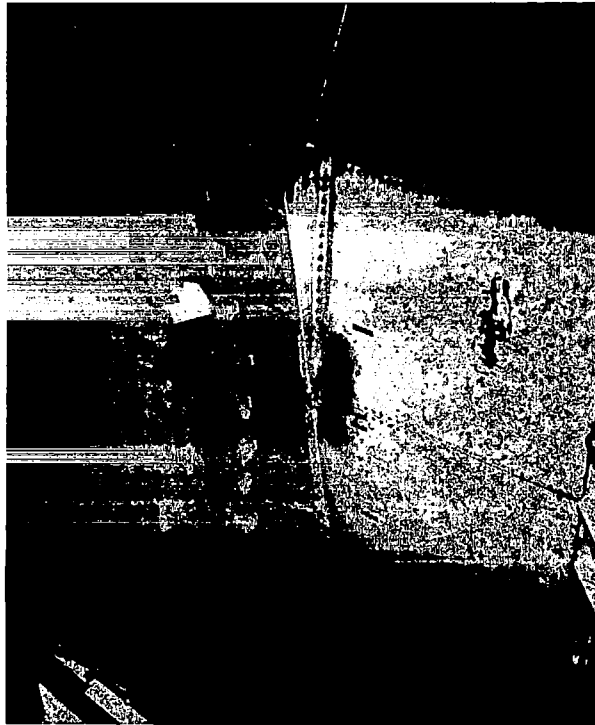


Figure 9.
Specimen #1.
Static test,
lower surface.
Failure at WS 176L.



Figure 10.
Specimen #1.
Static test,
lower surface.
Close-up of failure
near aft wing spar.

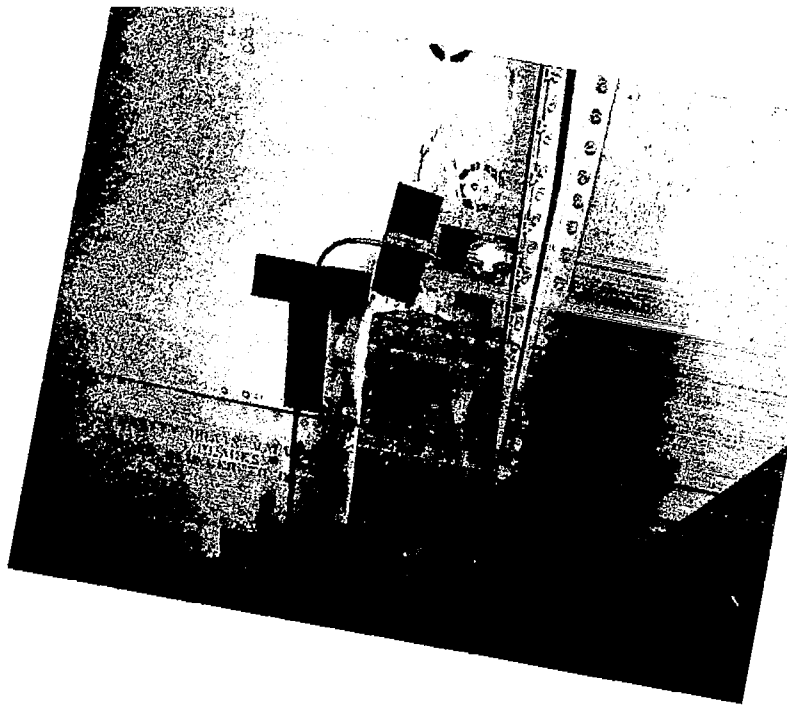


Figure 11.
Specimen #2.
Static test,
lower surface.
Initial skin damage
at WS 176L over
Stringer 16.

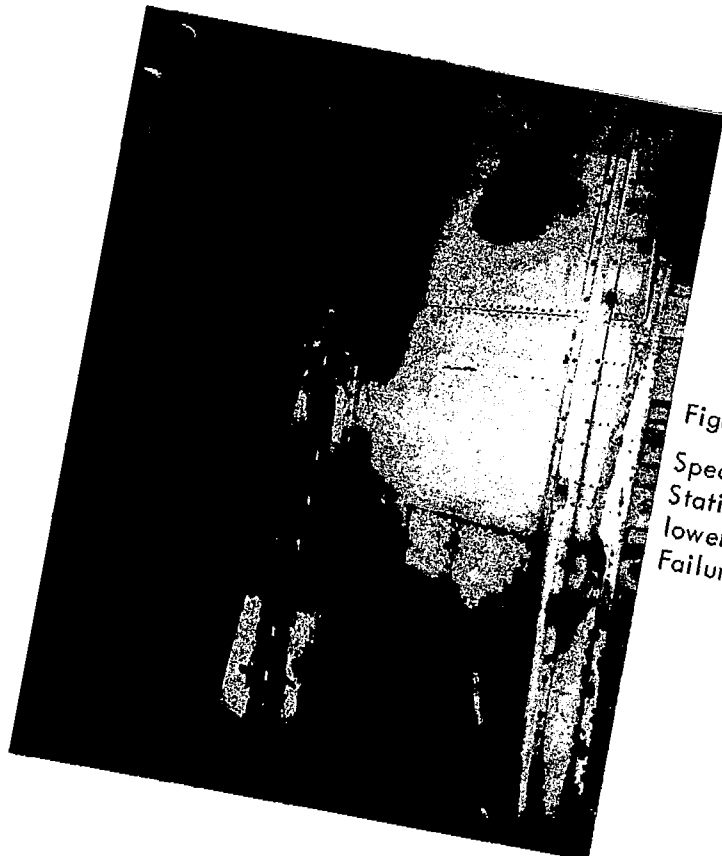


Figure 12.
Specimen #2.
Static test,
lower surface.
Failure at WS 176L.



Figure 13.
Specimen #3.
Static test,
lower surface.
Initial skin cracking
at WS 176R over
Stringers 15 and 16.



Figure 14.
Specimen #3.
Static test,
lower surface.
Second view of
initial skin cracking
at WS 176R over
Stringers 20 and 21.

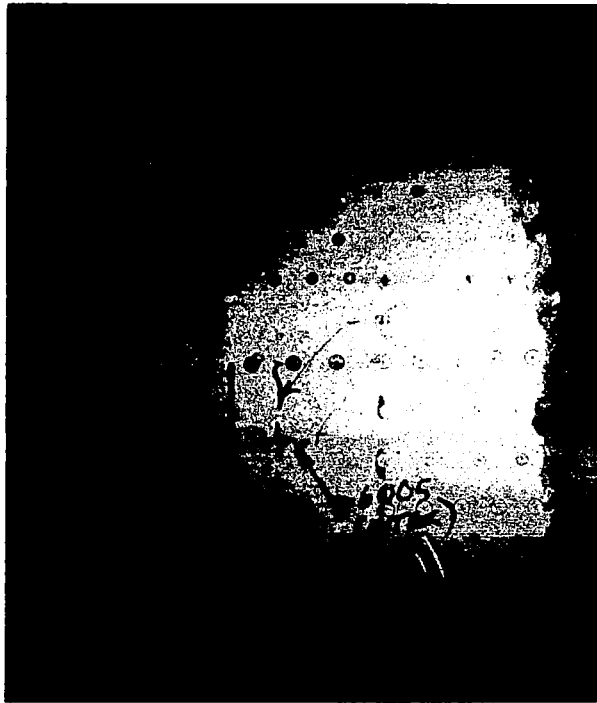


Figure 15.
Specimen #6.
Static test,
upper surface.
Final cracking at
WS 34.5L.

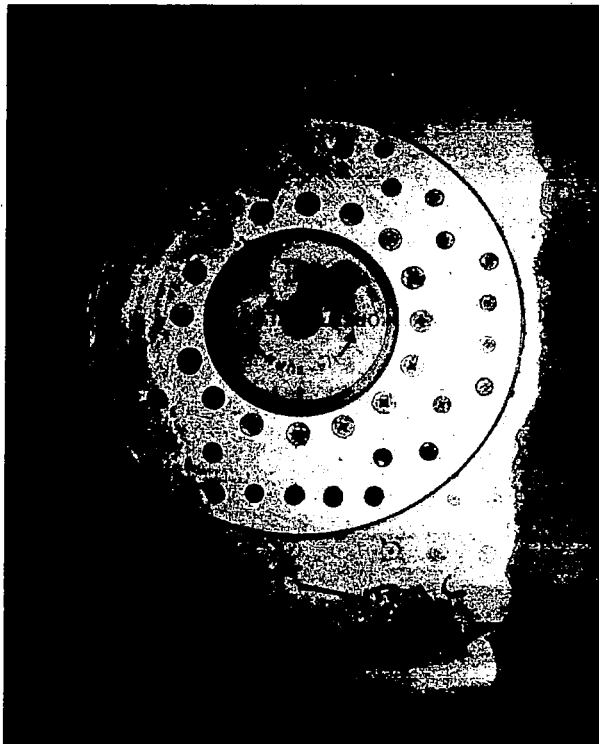


Figure 16.
Specimen #6.
Static test,
upper surface.
Final cracking
at WS 120.5
fuel filler hole.

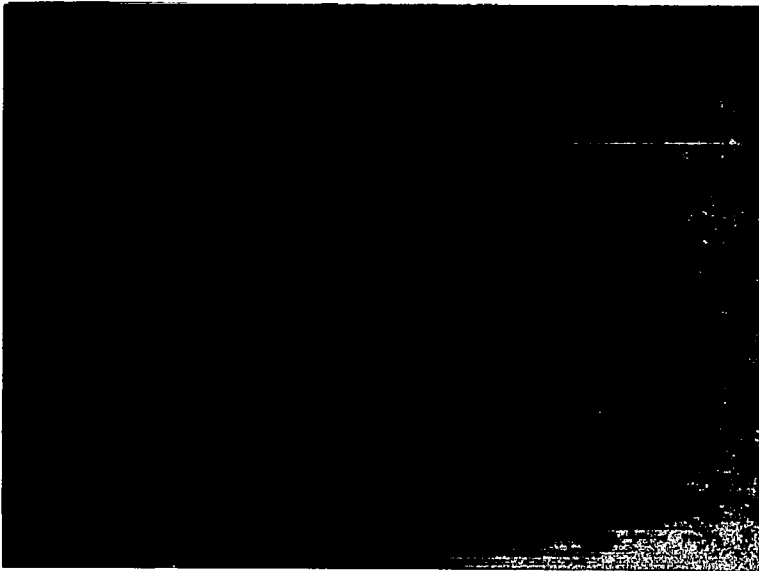


Figure 17.
Specimen #7.
Static test,
upper surface.
Final cracking at
WS 120.5R fuel
filler hole.

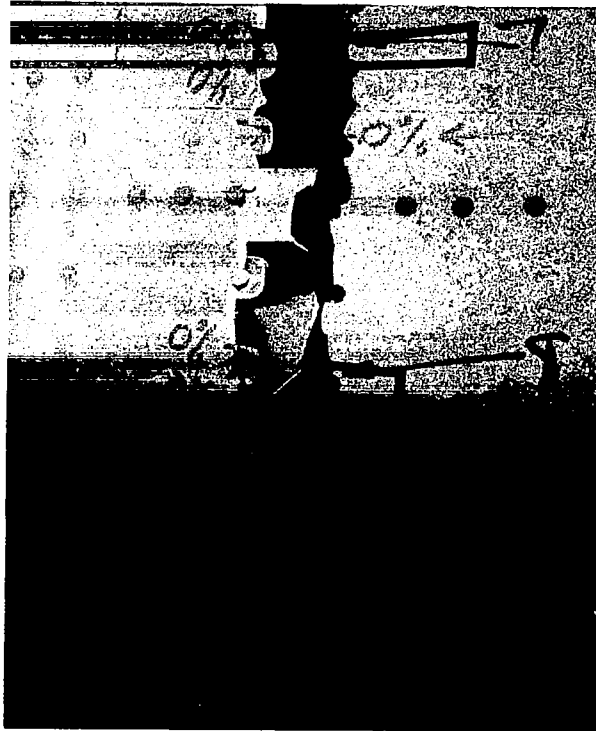


Figure 18.
Specimen #7.
Static test,
upper surface.
Close-up of
failure at
WS 135R.

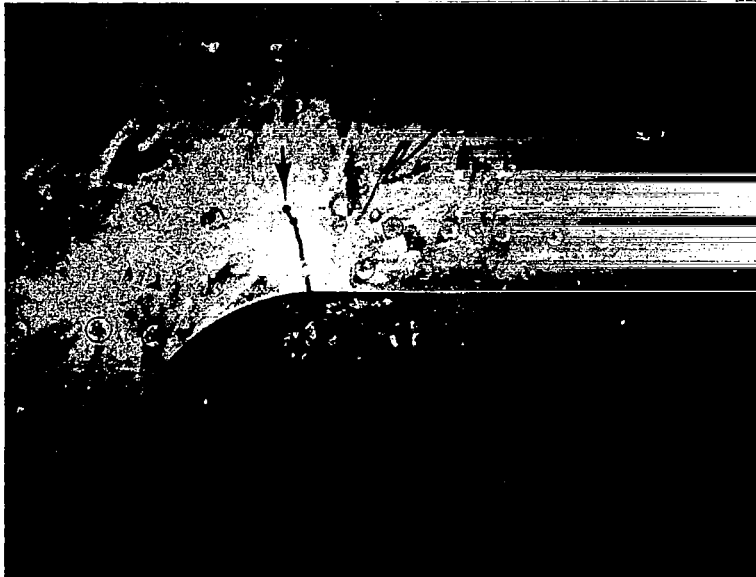


Figure 19.

Specimen #8.
Static test,
upper surface.
Initial crack at
corner of access
door, WS 182R.



Figure 20.

Specimen #8.
Static test,
upper surface.
Initial crack at
corner of access
door, WS 200L.



Figure 21. Specimen #8.
Static test, upper surface.
Initial crack at corner of
access door, WS 182L.

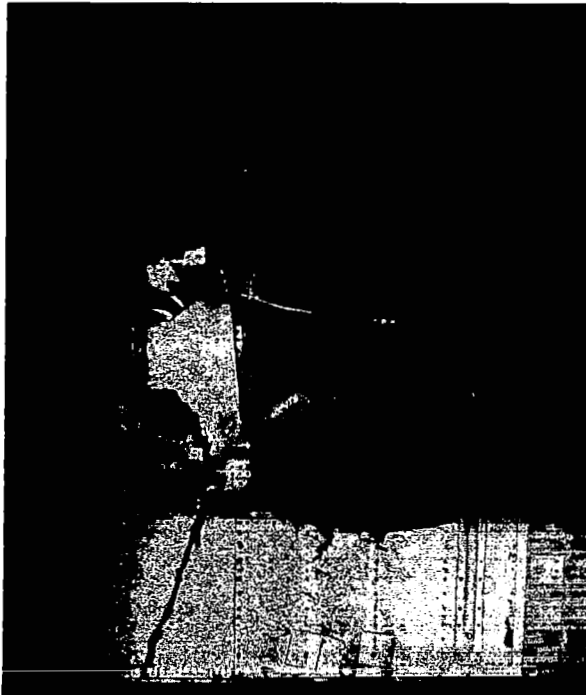


Figure 22.
Specimen #4.
Cyclic & static testing,
lower surface.
Overall view of failure
at WS 176L - 168L.

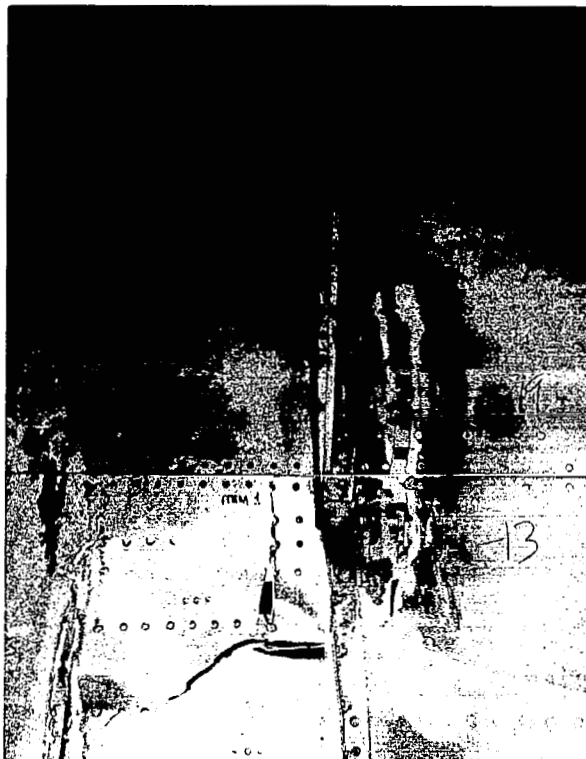


Figure 23.
Specimen #4.
Cyclic & static testing,
lower surface.
Close-up view of failure
near stringers 15 and 16.

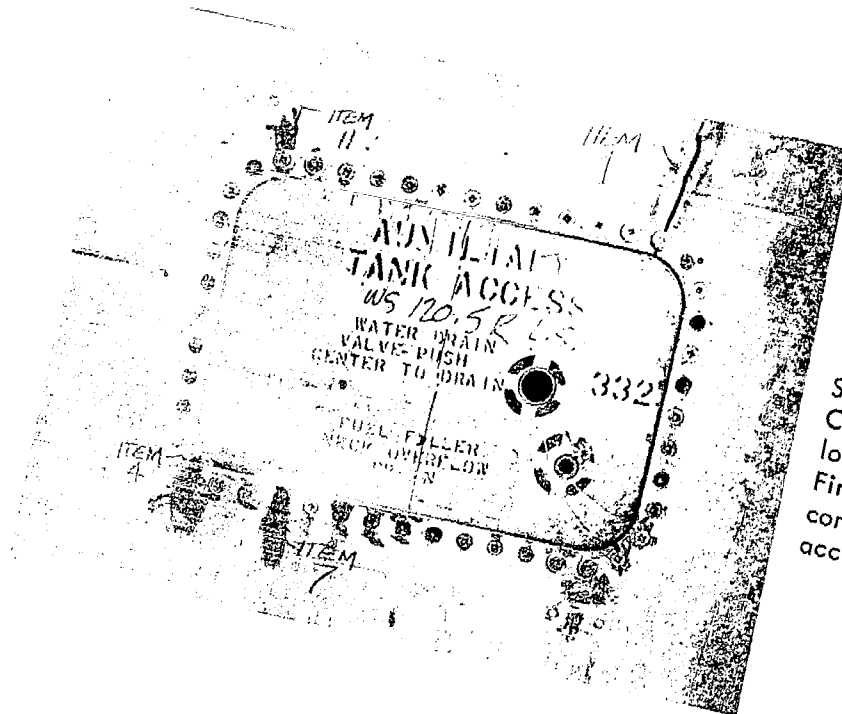


Figure 24.
Specimen #5.
Cyclic & static testing,
lower surface.
Final cracking at
corners of WS 120.5R
access door.

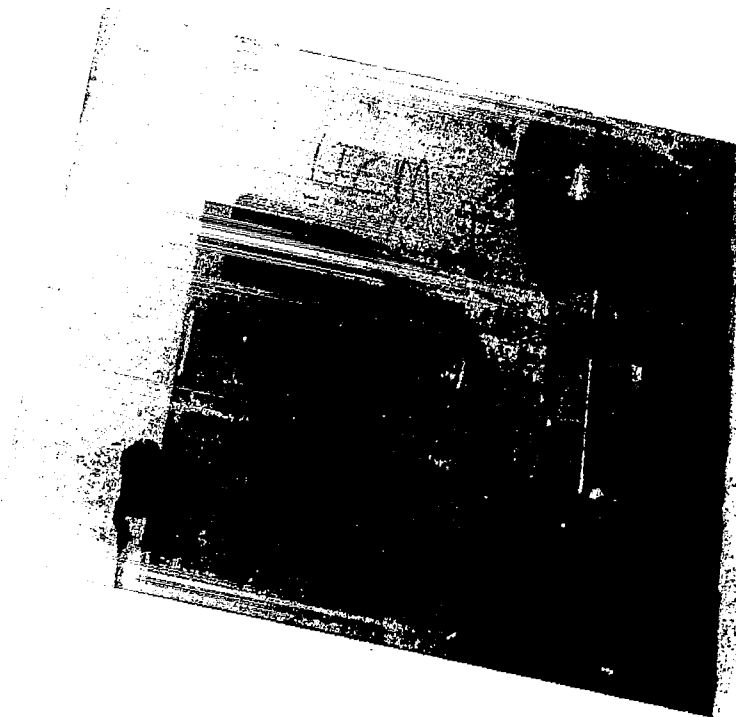


Figure 25.
Specimen #5.
Cyclic & static testing,
lower surface.
Crack at rainbow fitting
node, WS 220L, after
7000 cycles.



Figure 26.
Specimen #5.
Cyclic & static testing,
lower surface.
Failure at rainbow
fitting, WS 220R.



Figure 27.
Specimen #5.
Cyclic & static testing,
lower surface.
Final crack propagation
at WS 168L.

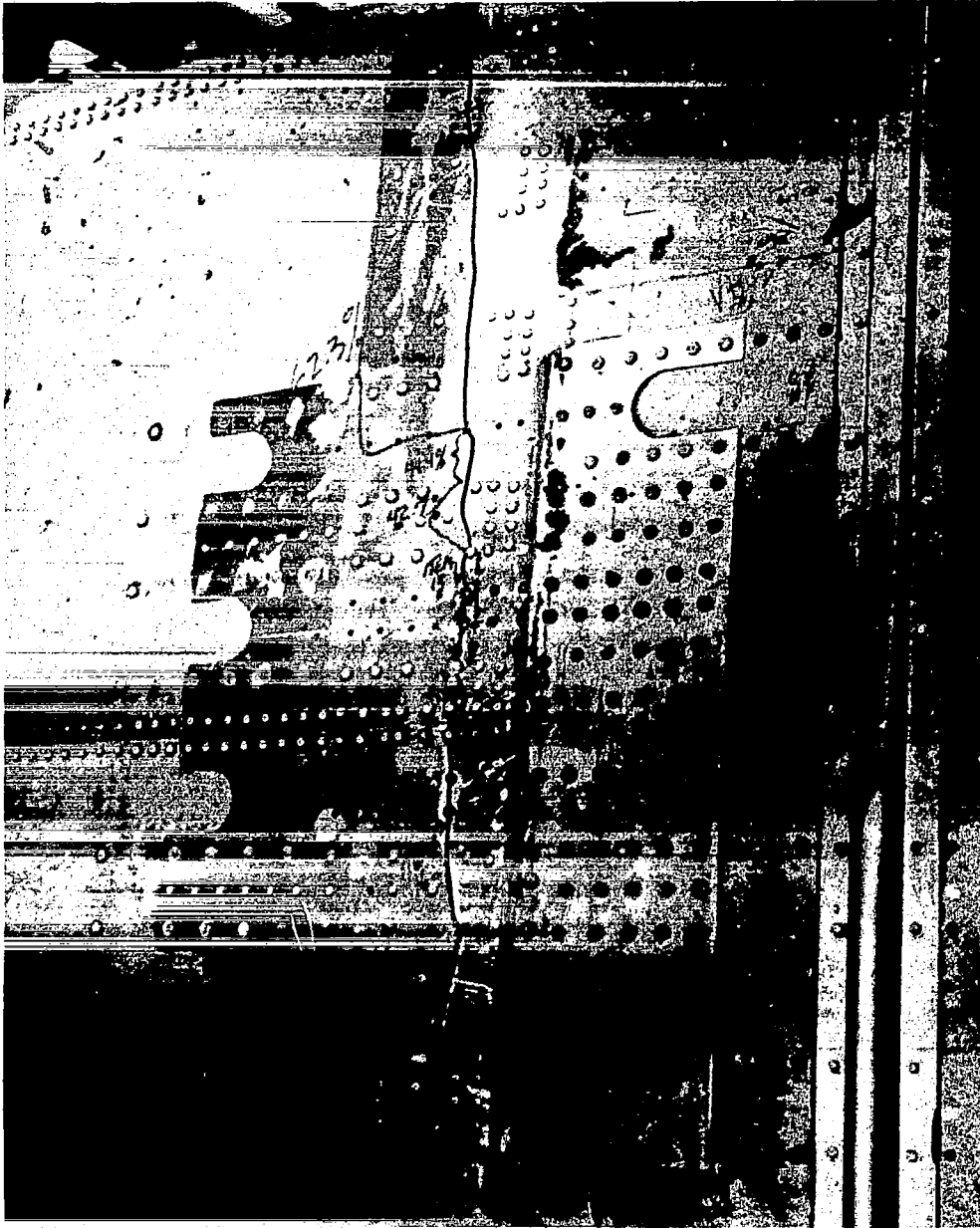


Figure 28. Specimen #13.
Cyclic & static testing, lower surface.
Repair patch removal and crack propagation,
WS 58L, forward region - final damage.

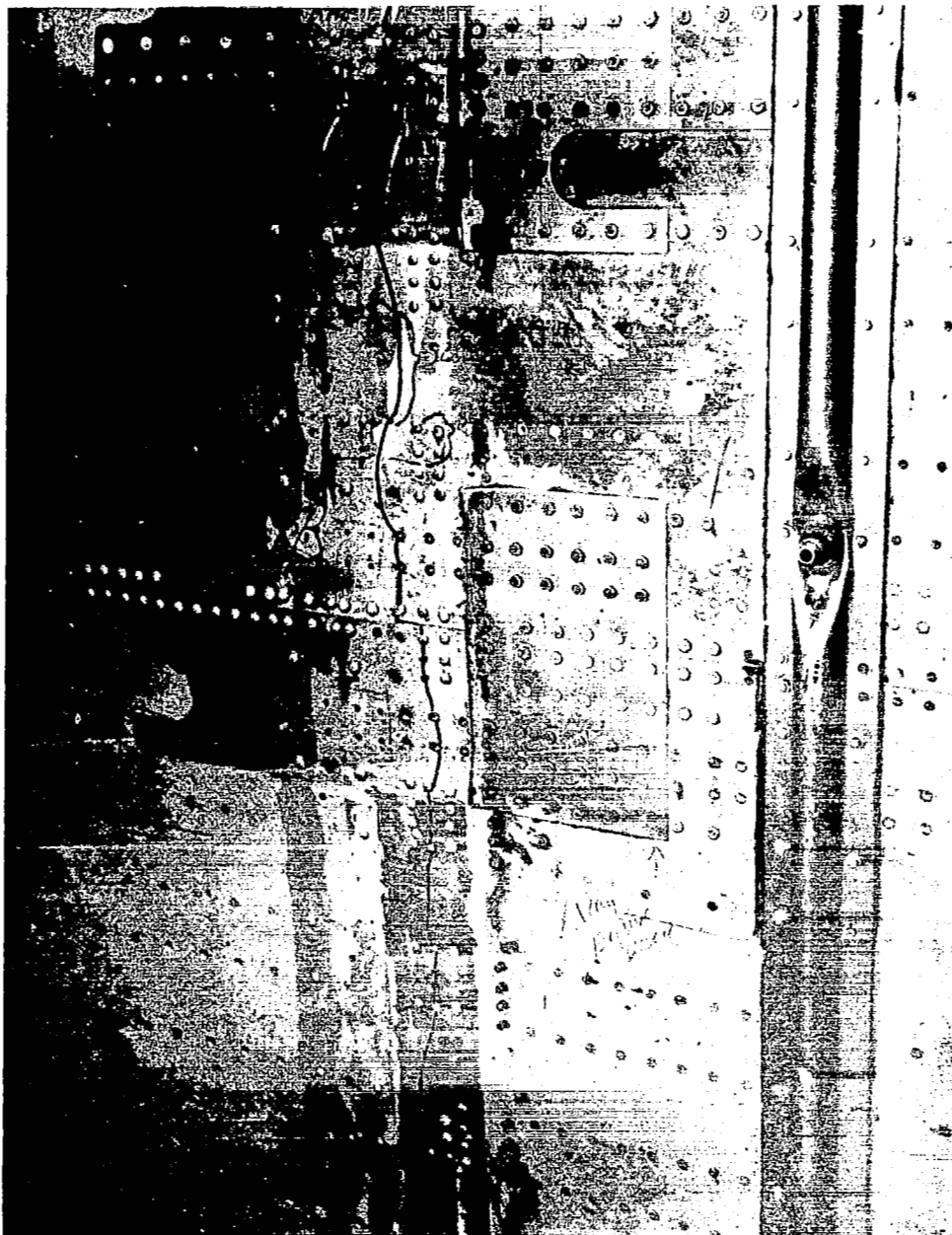


Figure 29. Specimen #13.
Cyclic & static test, lower surface.
Repair patch removal and crack propagation,
WS 58L, aft region - final damage.

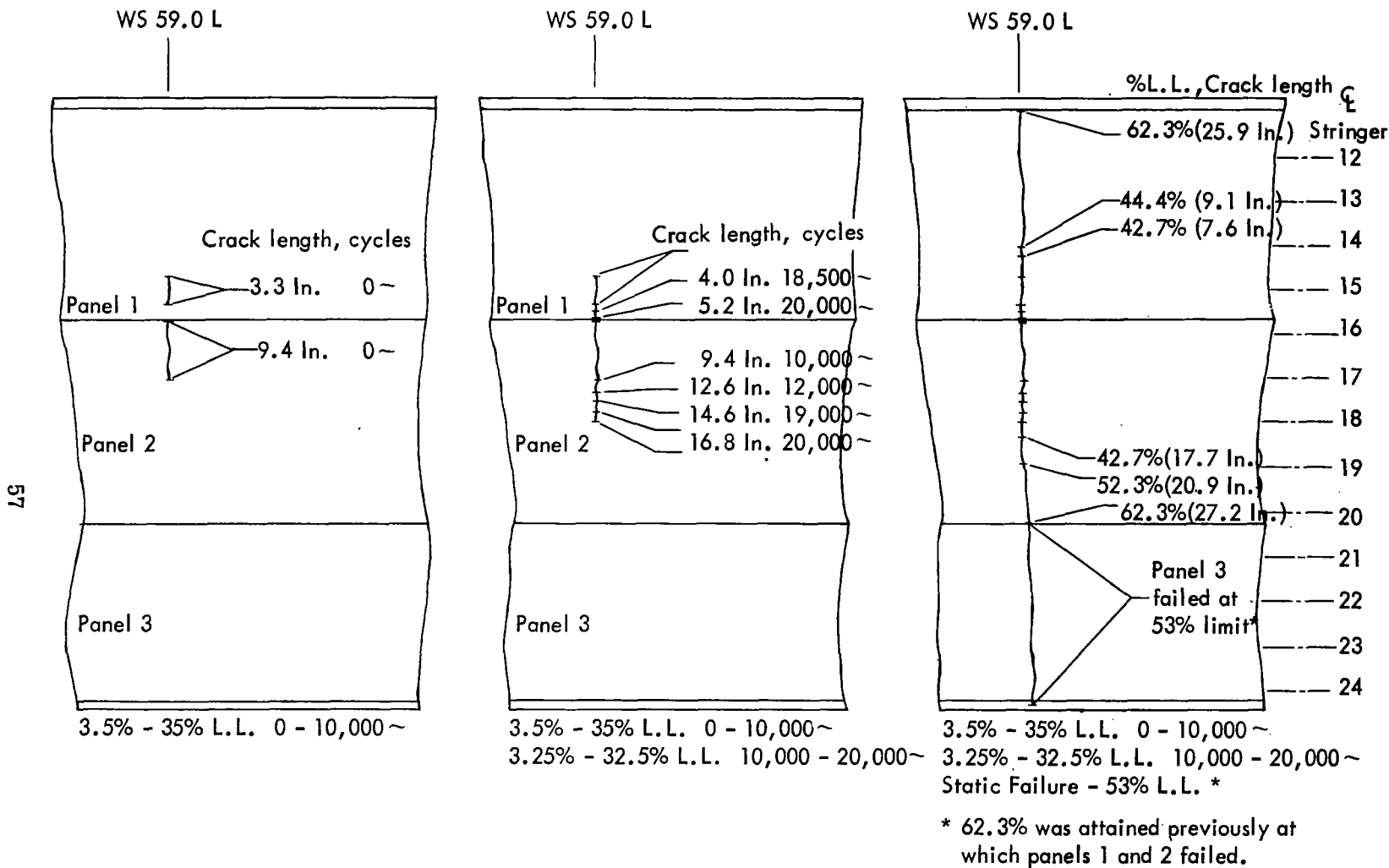


Figure 30 - Test specimen #13, progression of crack propagation to failure at W.S. 59L.

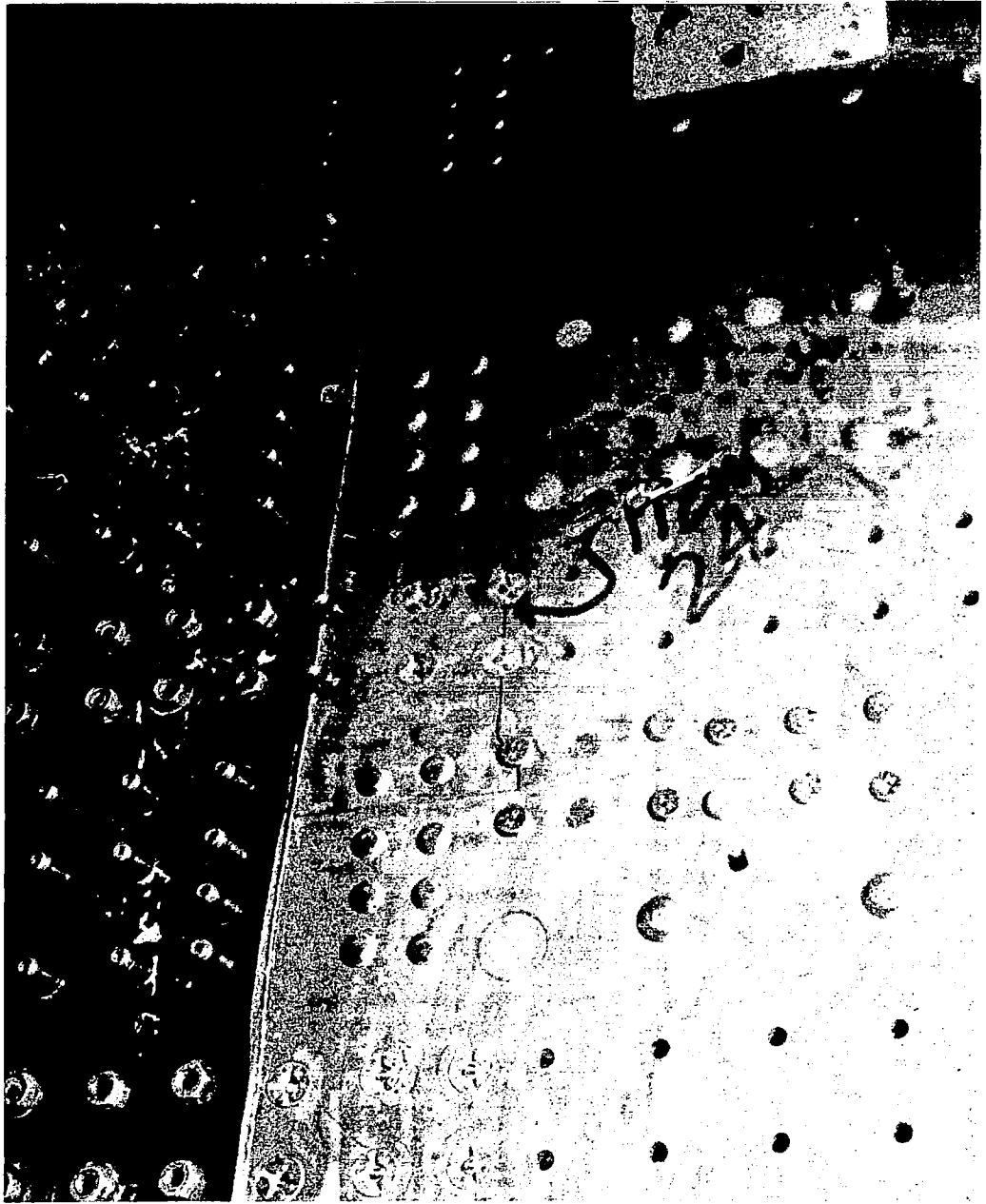


Figure 31. Specimen #14.
Cyclic & static test, lower surface.
Largest initial crack was 5.3 inches
at WS 58R.

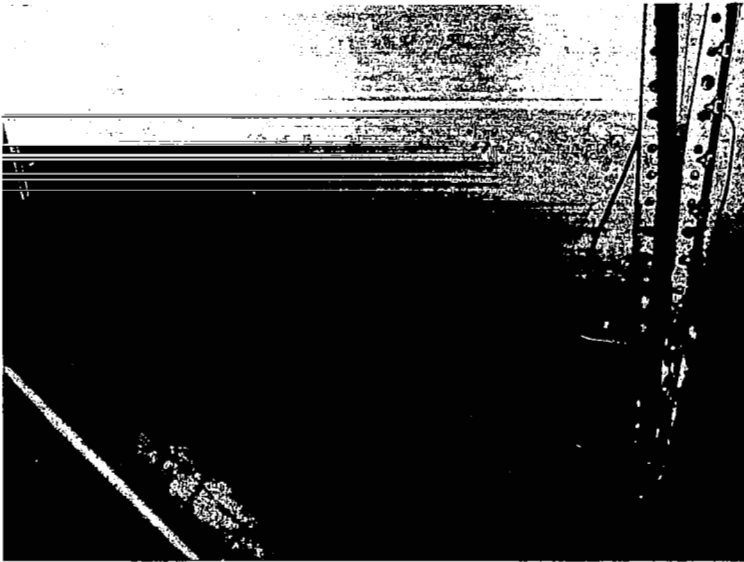


Figure 32.

Specimen #14.
Cyclic & static test,
lower surface.
Long crack along thrust angle,
forward region, WS 179R -
damage after test cycling.

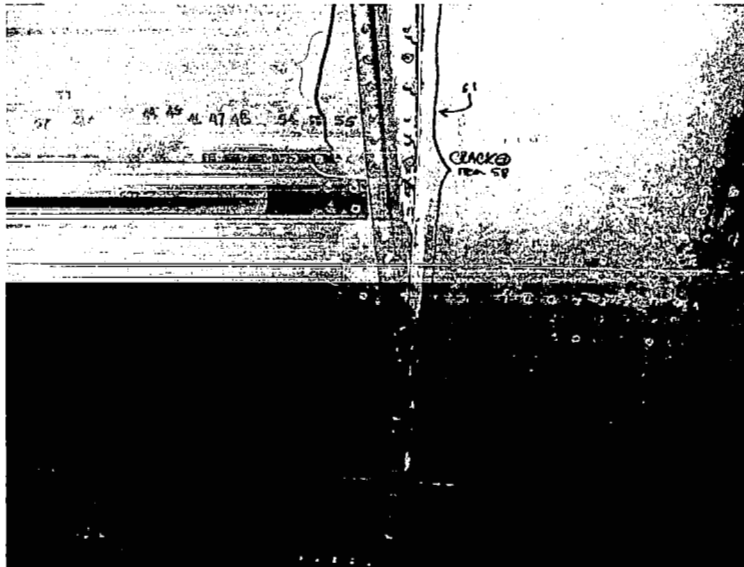


Figure 33.

Specimen #14.
Cyclic & static test,
lower surface.
Long crack along thrust
angle, aft region, WS 179R -
damage after test cycling.

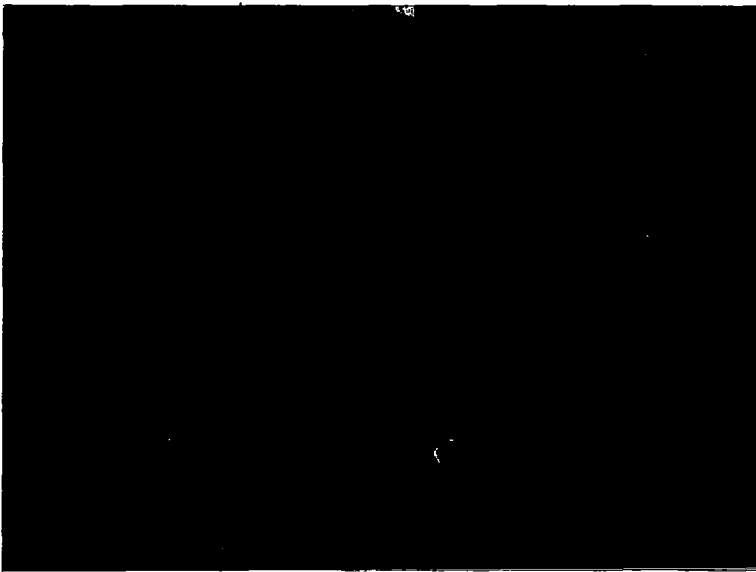


Figure 34.
Specimen #14.
Cyclic & static test,
lower surface.
Failure in vicinity of
WS 179R, note engine
thrust angle.

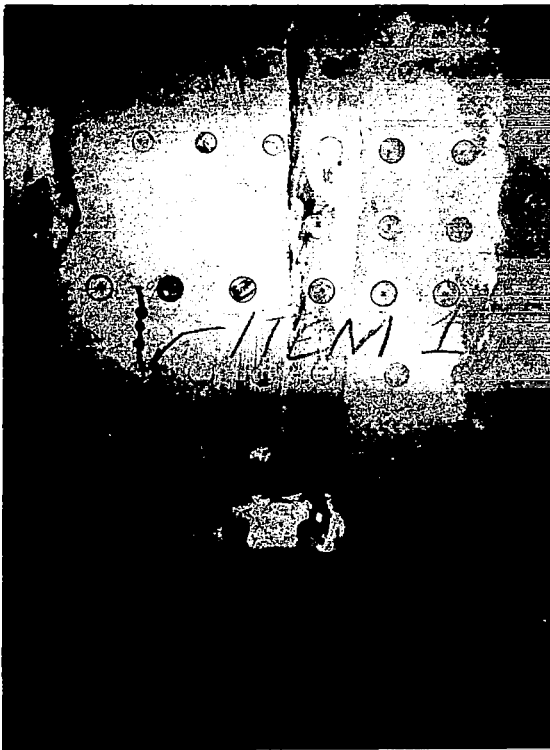


Figure 35. Specimen #9,
Cyclic & static test,
upper surface.
Initial crack of 3.6
inches at WS 34.5L.

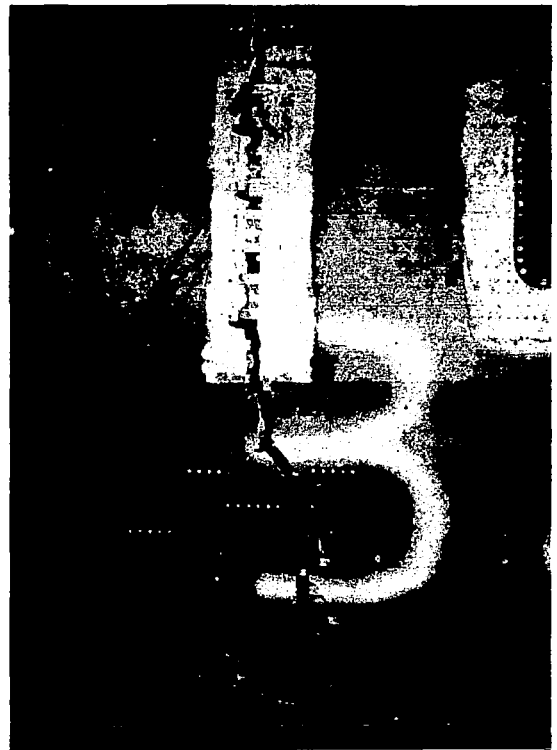


Figure 36. Specimen #9.
Cyclic & static test,
upper surface.
Failure at WS 34.5L.

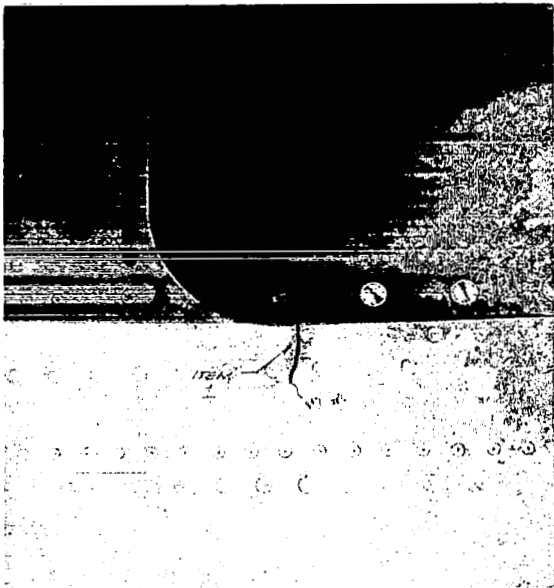


Figure 37.
Specimen #10.
Cyclic & static test,
upper surface.
Final crack at
corner of access
door, WS 198.5L.

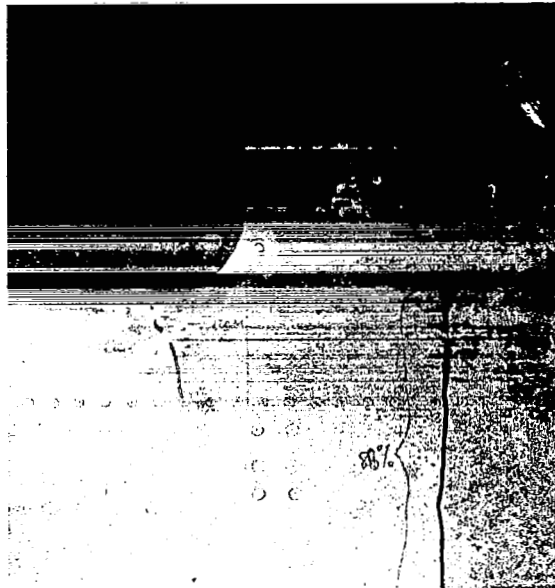


Figure 38.
Specimen #10.
Cyclic & static test,
upper surface.
Final crack at
corner of access
door, WS 182L.

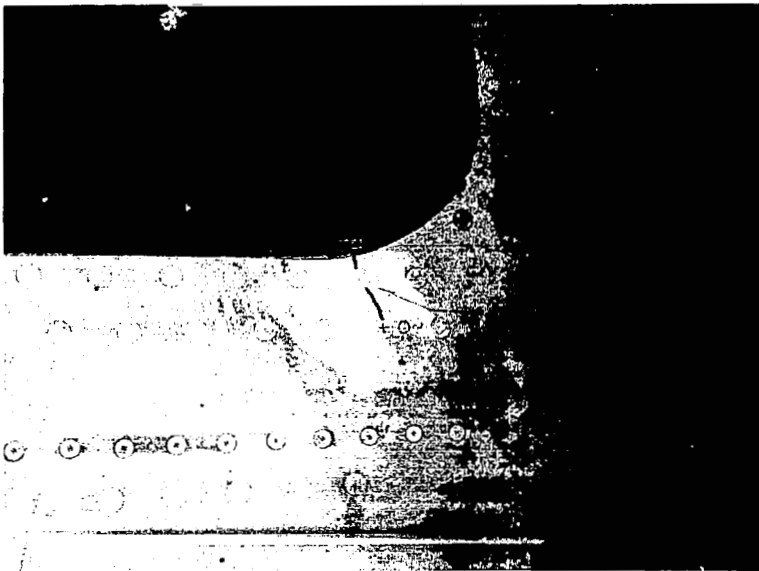


Figure 39.
Specimen #10.
Cyclic & static test,
upper surface.
Final crack at corner
of access door, WS 199R.



Figure 40.
Specimen #10.
Cyclic & static test,
upper surface.
Cracking in forward
region, WS 61L -
after cyclic testing.



Figure 41.
Specimen #10.
Cyclic & static test,
upper surface.
Cracking in aft
region, WS 61L -
after cyclic testing.



Figure 42.
Specimen #10.
Cyclic & static test,
upper surface.
Crack at WS 165R -
final damage.

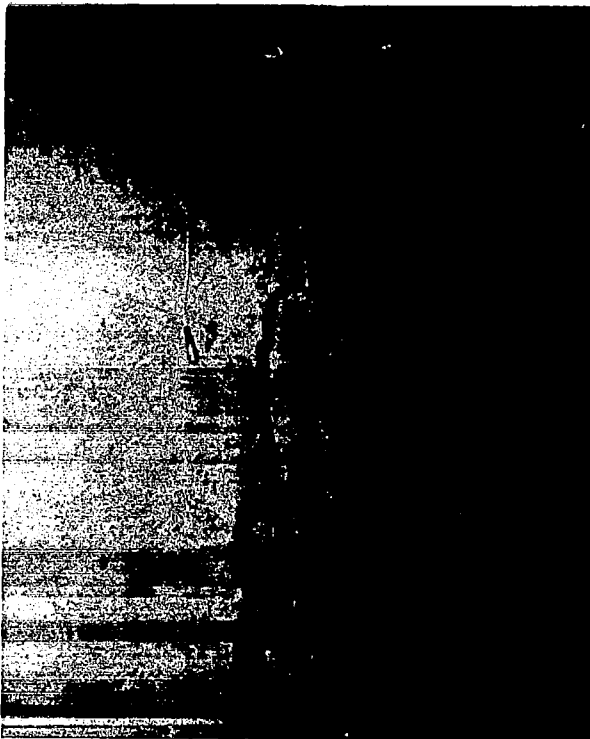


Figure 43.
Specimen #10.
Cyclic & static test,
upper surface.
Failure at WS 61L.

Figure 44. Specimen #11.
Static & cyclic test,
upper surface.
Final crack at corner
of cutout, WS 182.5L.

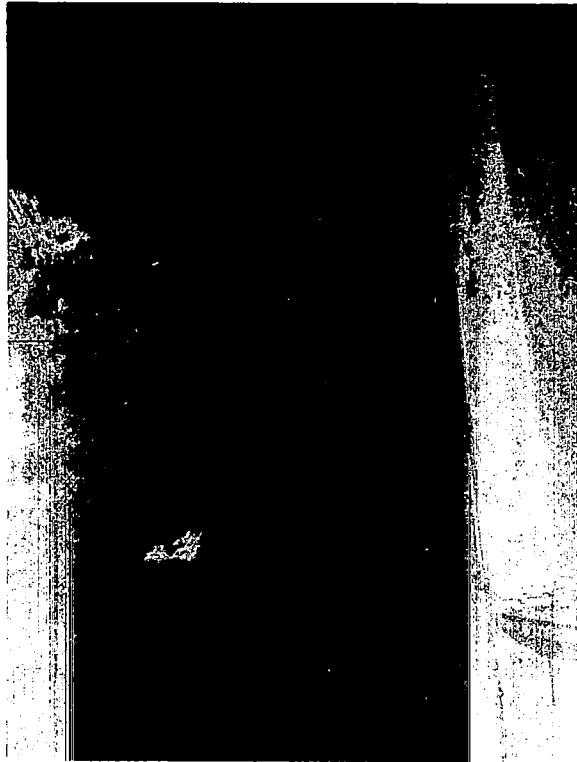


Figure 46.
Specimen #11.
Static & cyclic test,
upper surface.
Cracking along end
row of fasteners at
WS 213.5R - after
test cycling.

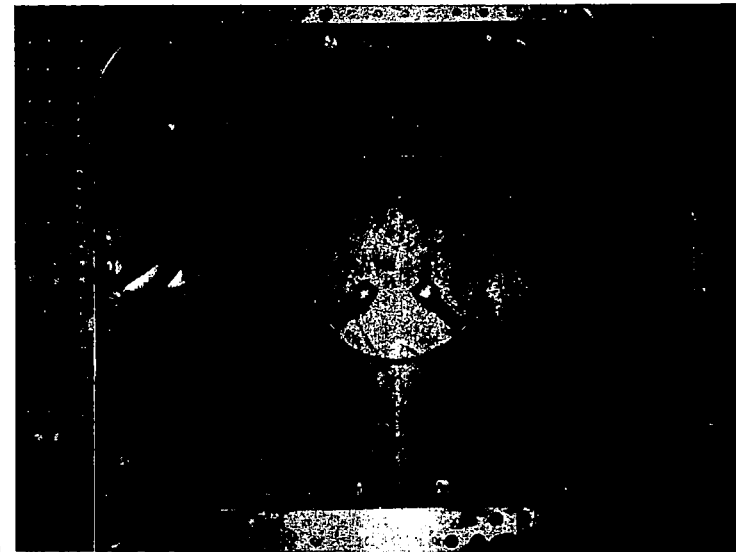
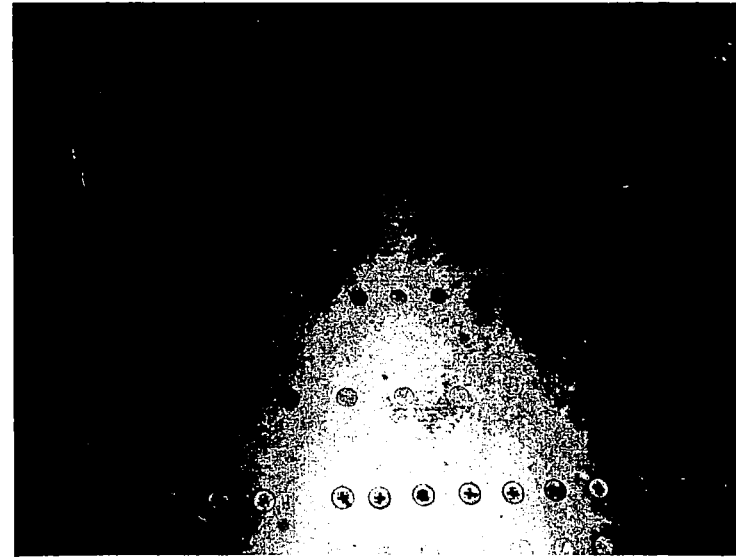


Figure 45.
Specimen #11.
Static & cyclic test,
upper surface.
Repair patches removed
from corners of cutout -
after test cycling.



Figure 47.
Specimen #12.
Static & cyclic test,
upper surface.
Cracking along end
row of fasteners at
WS 105L, panels #1
and #2 - after test
cycling.

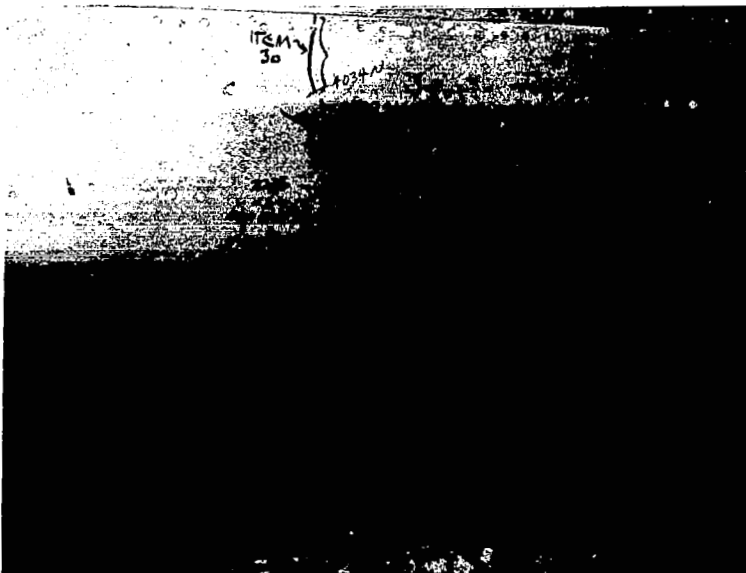


Figure 48.
Specimen #12.
Static & cyclic test,
upper surface.
Cracking at WS 105L,
panel #3 - after test
cycling.

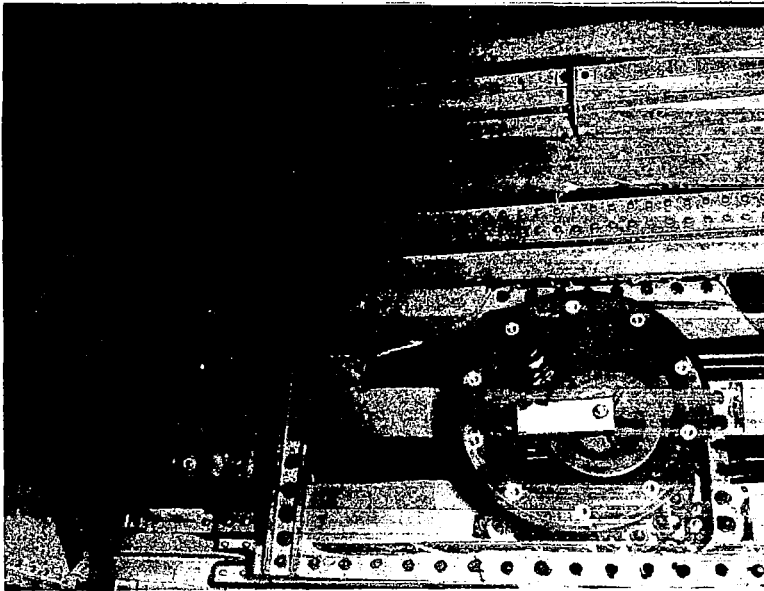


Figure 49.
Specimen #12.
Static & cyclic test,
upper surface.
Interior view of stringer
cracking, panels #1 and
#2, WS 105L - after test
cycling.

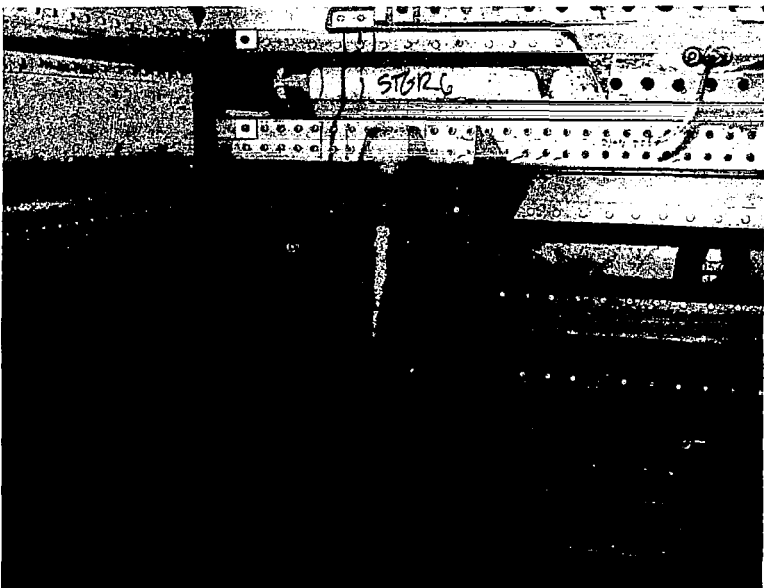


Figure 50.
Specimen #12.
Static & cyclic test,
upper surface.
Interior view of stringer
cracking, panels #2 and #
#3, WS 105L - after test
cycling.

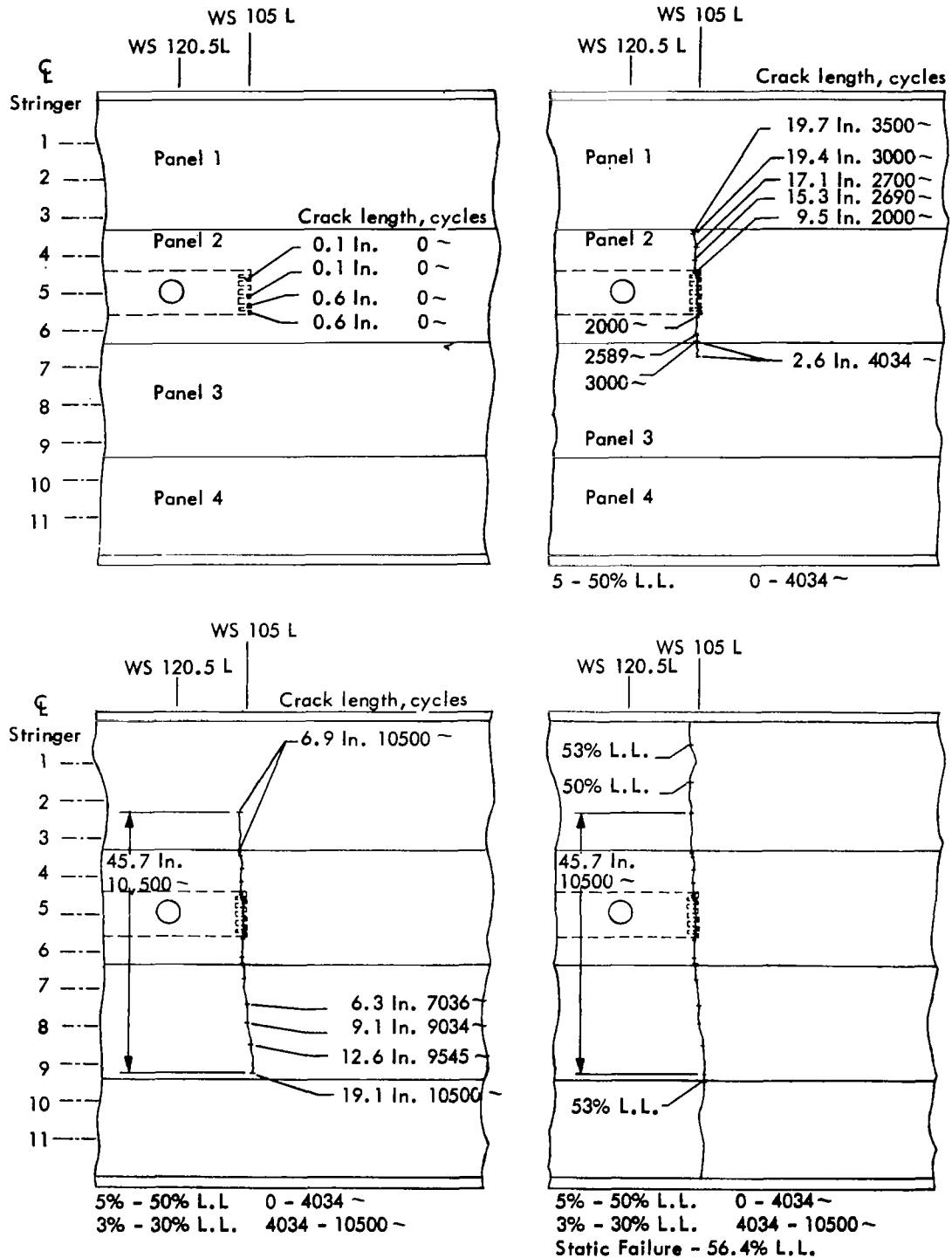


Figure 51. - Test specimen #12, progression of crack propagation to failure at W.S. 105 L.